SIGDEL, SUJATA. M.S. Synthesis and Analysis of Isomers of Unsaturated Hydrocarbon *Z*-Alkenes and Enantioselective Synthesis of Heterocycle via Desymmeterization. (2022) Directed by Dr. Kimberly S. Petersen. 60 pp.

Honeybees are the most important crop pollinators, and they play a major role in the natural ecosystem, scientific innovations, and food security. The health of honeybees is declining due in part to the ectoparasitic mite, *Varroa destructor* (*Varroa*). *Varroa* is a physical burden to honeybees because they feed on the fat body of the brood which negatively impacts the health of the honeybees. *Varroa* is a physiological burden to its host, but they can be reduced at the colony level through hygienic behavior, the detecting, uncapping, and removing of the diseased or infested brood from the hive by adult bees. The trigger for the hygienic behavior is a chemical signal composed primarily of monoalkenes and produced by unhealthy brood. Numerous hydrocarbons have been associated with unhealthy broods, some of which have shown to trigger hygienic behavior. Some hygiene-inducing compounds have been identified as *Z*-6 C_{15}, *Z*-8 C_{17}, *Z*-8 C_{31}, and *Z*-10 C_{33} and are elevated in *Varroa*-infested brood. Hydrocarbons C_{25} and C_{27} have also been known to be associated with unhealthy brood, and recently, the double bond location of the most prominent isomers of C_{25} and C_{27} have been identified. The *Z*-9 isomers of C_{25} and C_{27} are found to be a dominant form found in honeybees and are predicted as most biologically active. *Z*-7 of C_{25} and C_{27} have also been identified in honeybees but in a smaller quantity and *Z*-8 of C_{25} and C_{27} have not been previously identified in honeybees, however, its presence is a possibility. This project focuses on synthesizing the *Z*-isomers of C_{25} and C_{27} (*Z*-7, *Z*-8, and *Z*-9) with greater than 95% purity. After the synthesis, these compounds will be tested for biological activity related to hygienic behavior in future field research.

Enantioselective synthesis is a key subject in modern chemistry and often important in the field of pharmaceuticals. Enantioselective synthesis is a form of chemical synthesis in which one enantiomer of the chiral product is produced preferentially. Enantiomers are mirror image stereoisomers that are a non-superimposable. A set of two different enantiomers of molecules have different biological activities and functions. A desymmetrization reaction involves a modification where a molecule loses one or more symmetrical features. It is also a technique to synthesize enantiomers. Previous works in Dr. Petersen's group have dealt with desymmetrization of malonic ester derivatives in the presence of chiral Brønsted acid catalyst to achieve enantioenriched heterocycles. The goal of this project is to use a Knoevenagel condensation, hydrogenation, and cyclization reaction catalyzed by chiral Brønsted acid catalyst to achieve an enantioselective product.

SYNTHESIS AND ANALYSIS OF ISOMERS OF UNSATURATED HYDROCARBON Z-ALKENES AND ENANTIOSELECTIVE SYNTHESIS OF HETEROCYCLE VIA DESYMMETRIZATION

by

Sujata Sigdel

A Thesis

Submitted to

the Faculty of The Graduate School at

The University of North Carolina at Greensboro

in Partial Fulfillment

of the Requirements for the Degree

Master of Science

Greensboro

2022

Approved by

Dr. Kimberly S. Petersen
Committee Chair

APPROVAL PAGE

This thesis written by Sujata Sigdel has been approved by the following committee of the Faculty of The Graduate School at The University of North Carolina at Greensboro.

Committee Chair

Dr. Kimberly S. Petersen

Committee Members

Dr. Kaira Wagoner

Dr. Mitchell Croatt

May 19, 2022

Date of Acceptance by Committee

May 19, 2022

Date of Final Oral Examination

ACKNOWLEDGEMENTS

Thank you, Dr. Kimberly Petersen, for giving me an opportunity to conduct research in Organic synthesis and for guidance and patience. Thank you, Dr. Kaira Wagoner, for giving me an opportunity to become part of your research with Honeybees. Thank you, Dr. Mitchell Croatt, for the time and support as a committee member. Thank you, Dr. Franklin Moy for the training on the NMR instrument and for sharing knowledge of NMR. Thank you, Dr. Daniel Todd, for providing training on the GC-MS instrument and providing GC-MS analysis of samples. I thank Tyler Greenstein for his time and effort in providing training on laboratory techniques used in organic synthesis. I thank other members of the Petersen research group for assistance and constructive feedback.

TABLE OF CONTENTS

LIST OF TABLES vi

LIST OF FIGURES vii

CHAPTER I: HONEYBEE AND HYGENIC BEHAVIOR INTRODUCTION 1

Hygienic Behavior 1

Hydrocarbons and Honeybees 2

Previous Identified Active Compounds 3

CHAPTER II: SYNTHESIS OF HYDROCARBON *Z*-ALKENES 5

Present Work 5

Future Work and Conclusion 13

CHAPTER III: HETEROCYCLE FORMATION INTRODUCTION 15

Stereoisomers 15

Indole-Containing Compounds 16

Brønsted Acid Catalysts 18

Previous Work of Dr. Petersen Group 20

CHAPTER IV: CARBON-CARBON BOND FORMATION PRODUCING ENANTIOSELECTIVE HETEROCYCLE 23

Present Works 23

Future Works and Conclusion 27

CHAPTER V: EXPERIMENTAL PROCEDURES AND METHODS 29

General Information 29

Synthesis of Octadecanal (2) 29

Synthesis of Heptadecanal (5) 30

Synthesis of Hexadecanal (8) 31

Synthesis of Eicosanal (11) 31

Synthesis of Nonadecanal (14) 32

Synthesis of *Z*-7 C_{25} (3) 33

Synthesis of *Z*-8 C_{25} (6) 33

Synthesis of *Z*-9 C_{25} (9) 34

Synthesis of *Z*-7 C_{27} (12) 35
Synthesis of *Z*-9 C_{27} (16) 36
Synthesis of 19 36
Synthesis of 20 37
Synthesis of 21 38
REFERENCES 39
APPENDIX A: NMR SPECTRA 42
APPENDIX B: GAS CHROMATOGRAPHY MASS SPECTROMETRY 53
APPENDIX C: GAS CHROMATOGRAPHY 57

LIST OF TABLES

Table 1. Summary of Alkene Synthesis with Amounts Prepared Purity of Compounds and Percent Yields. 13

LIST OF FIGURES

Figure 1. Two-Step Synthesis; Oxidation Reaction and Wittig Reaction 5

Figure 2. Oxidation Reaction 5

Figure 3. Mechanism of Oxidation Reaction using Dess-Martin Periodinane as a Reagent. 6

Figure 4. Reaction Scheme of Preparation of Aldehyde Compounds. 7

Figure 5. Wittig Reaction. 8

Figure 6. Mechanism of Wittig Reaction. 8

Figure 7. Wittig Reaction for Synthesis of Z9-C25. 9

Figure 8. Wittig Reactions for Synthesis of *Z*-7 C25, *Z*-8 C25, *Z*-7 C27, *Z*-8 C27, and *Z*-9 C27, respectively. 10

Figure 9. GC Result to Show Formation of Byproduct (13.921) and Product (17.845) Peaks for Compound 9 11

Figure 10. EI Spectra of the Byproduct of Compound 9 12

Figure 11. Putative Mechanism for Dimerization of Nonyl-triphenyl Phosphonium Bromide. .. 12

Figure 12. Bromochlorofluoromethane Chiral Molecule. 16

Figure 13. Rotation of Molecule A about 180° with Attempt to Superimpose Molecules A and B. 16

Figure 14. Fischer Indole Synthesis Reaction. 17

Figure 15. L-Tryptophan and Four Ergot Alkaloid Types- D-Lysergic Acid, Lysergic Acid Amide, Argoclavine, and Ergotamine. 18

Figure 16. p-Toluenesulfonic Acid, Methanesulfonic Acid, and (R)-TRIP Catalyst. 19

Figure 17. Proposed Activation Complex Between (R)-TRIP Catalyst and Malonic Ester. 20

Figure 18. Work Accomplished by Dr. Jennifer Wilent. 21

Figure 19. Work Accomplished by Dr. Amber Kelly 22

Figure 20. Proposed Synthetic Pathway for Formation of Compound 21. 24

Figure 21. Knoevenagel Condensation Reaction. 25

Figure 22. Proposed Mechanism of Knoevenagel Condensation. 25

Figure 23. Hydrogenation Reaction of Compound 20. 26

Figure 24. Proposed Desymmetrization Reaction of Compound 20 in the Presence of Brønsted Acid. 27

Figure 25. Failed Attempt to Desymmetrize Compound 20 in Presence of p-Toluenesulfonic Acid. 27

CHAPTER I: HONEYBEE AND HYGENIC BEHAVIOR INTRODUCTION

Hygienic Behavior

The ectoparasitic mite *Varroa destructor* causes severe damage to honeybee health and is considered as one of the main threats for the bee keeping industry[1]. *Varroa,* originated from Asian honeybee (*Apis cerana*), is considered a threat to the western honeybee (*Apis mellifera*).[2] For reproduction, *Varroa* enter the uncapped cell and conceal themselves at the base of the cell in the brood food. Once the food has been consumed by the brood, *Varroa* emerge and feed on the fat body of the brood.[3] The fat body is essential to honeybee survival and losing the fat body tissue weakens honeybee's ability to detoxify pesticides and deprives them of vital food stores.[4] *Varroa* feeding on the fat body is harmful to honeybee health and can lead of decrease in body weight and protein levels.[5]

Varroa increases susceptibility of honeybee to viruses, which contributes to the deterioration of honeybee health. Deformed wing virus (DWV), a positive, single stranded RNA virus, is vectored by *Varroa,* and can cause deformed wings, shortened abdomen, reduced weight, discoloration, and premature death in honeybees.[6] When DWV occurs in the presence of *Varroa*, it is deemed as a substantial contributor to the decline in the health of honeybee.[7]

Honeybees are vulnerable to *Varroa* and DWV because they are social insects, and thus frequently in contact with the genetically similar nestmates. To prevent colony loss and control *Varroa*, various interventions such as chemical treatments like organic acids and essential oils and mechanical techniques like use of *Varroa*-resistant honeybee stocks exists.[8] One promising strategy for pest and disease control in honeybee colonies is the selection of hygienic honeybees that demonstrate an enhanced ability to detect and remove unhealthy brood from the colony. Hygienic behavior is a heritable trait [2] and selective breeding of mite resistant honeybees such as

Varroa Sensitive Hygienic (VSH) and Minnesota Hygienic (HYG) stocks have showed higher level of hygienic behavior [2] and show more resistance to *Varroa* mite compared to unselected colonies. However, there are numerous methods for breeding hygienic bees, and hygienic performance does not always confer *Varroa* resistance.[8] The selective breeding of hygienic bees tends to trade efficacy for efficiency because achieving high level of Varroa-specific hygiene is time consuming and require greater technical skills.[8] Hygienic behavior is an age-specific sanitary activity which is most commonly observed in 15-20 days old worker bees, and that is triggered in response to olfactory chemicals released by stressed brood.[9]

Hydrocarbons and Honeybees

In honeybees and other insects, hydrocarbons like alkanes, alkenes, and methyl alkanes are found on the cuticles and function to prevent desiccation and facilitate communication.[10] Hydrocarbons are naturally occurring organic compounds composed exclusively of carbon and hydrogen atoms. They have a carbon-chain skeleton and hydrogens are attached to the carbon skeleton and can be saturated as well as unsaturated. Saturated hydrocarbons, such as alkanes, are compounds in which all carbon-carbon bonds are single bonds and have a general formula of C_nH_{2n+2}. Unsaturated hydrocarbons contain double or triple bonds such as an alkenes or an alkynes and have general formula of C_nH_{2n} for alkenes and C_nH_{2n-2} for alkynes. Hydrocarbons can be straight chained or branched chain with the same empirical formula but can show differences in the properties. The physical properties of unsaturated hydrocarbons are non-polar and relatively insoluble in water. The intermolecular bonds are weak van der Waals bonds. Larger and heavier hydrocarbon chains have higher melting point as well as boiling points.

The biosynthesis of hydrocarbon on honeybees occurs in the oenocytes in which the first step is elongation of fatty acids, followed by reduction of the fatty acids to aldehydes, and finally

conversion of aldehydes to hydrocarbons by losing the carbonyl carbon.[11] The hydrocarbons are then transferred from oenocytes to the cuticles via hemolymph.[12] Hydrocarbons found in the cuticles of the honeybees are detectable by their nestmates and facilitate communication, including nestmate recognition and task performance. Hydrocarbon type and quantity when used in communication can be classified with varying levels of sensitivity for intra-colonial as well as inter-colonial recognition tasks.[13] Alkenes, as compared to alkanes, elicit stronger behavioral response[14] and can be discriminated by honeybee workers more easily. Honeybee health and hygienic behavior have been associated with many monoalkenes with similar structures but variety of volatilities. For hygiene communication, smaller, more volatile compounds attract workers, while larger, less volatile compounds could trigger hygienic behavior.[15] The less volatile cuticular hydrocarbons can also help workers pinpoint the location of compromised cells more accurately.[15]

Previous Identified Active Compounds

Vander Meer et al. provided the major review of social insect pheromones, and the paper has been used as a solid introduction to the field.[16] A potential path for the development of improved control of mites and pathogens is to facilitate selective breeding of *Varroa*-resistant honeybees. This is achieved through the identification and synthesis of hygiene-inducing compounds.[15] The hygiene-inducing compounds are active compounds that are naturally elevated in *Varroa*- parasitized brood.[15] Previously identified and synthesized active compounds are *Z*-6 C_{15}, *Z*-8 C_{17}, *Z*-8 C_{31}, and *Z*-10 C_{33}. A mixture of these compounds was used to test hygiene response associated and how it could serve as an improved tool for predicting colony level *Varroa* resistance. A mixture of active compounds were applied to the cell caps of honeybee brood and tested for a two-hour colony response.[17] These active compounds have

shown to be negatively correlated with the colony *Varroa* infestation.[17] A control mixture containing structurally similar compounds such as *Z*-7 C_{15}, *Z*-7 C_{17}, *Z*-15 C_{30}, and *Z*-16 C_{32} was used to compare the performance of the assay.[15] The control compounds were similar in sizes and structures to the hygiene-inducing compounds and have not been detected on honeybee cuticles.

Previously, Wagoner et al. (2020) have identified two hydrocarbons (C_{25} and C_{27})[15], that are associated with the unhealthy brood. The double bond location of the most prominent isomers has been recently identified by Dr. Jocelyn Millar. The dominant isomers of C_{25} and C_{27} were identified as *Z*-9 and predicted to be the most biologically active. However, these isomers have not yet been tested for hygienic behavior. Isomer *Z*-7 has been present in honeybees but in a smaller quantity and *Z*-8 isomer could be present in honeybees, however, it has not been identified previously in the honeybees. For this research, synthesis of six alkenes, *Z*-7 C_{25}, *Z*-8C_{25}, *Z*-9 C_{25}, *Z*-7 C_{27}, *Z*-8 C_{27}, and *Z*-9 C_{27} were performed to enable field tests of each compound's biological activity. This work facilitates the development of important selective breeding tools which will improve the health of honeybees and reduce honeybee colony death.

CHAPTER II: SYNTHESIS OF HYDROCARBON *Z*-ALKENES

Present Work

The first part of the project was to synthesize at least 500 mg of the required *Z*-isomers of C_{25} and C_{27} to be further tested in the field for biological activities. In order to achieve the goal of the research, a two-step synthesis was implemented, an oxidation reaction followed by Wittig reaction (Figure 1).

Figure 1. Two-Step Synthesis; Oxidation Reaction and Wittig Reaction

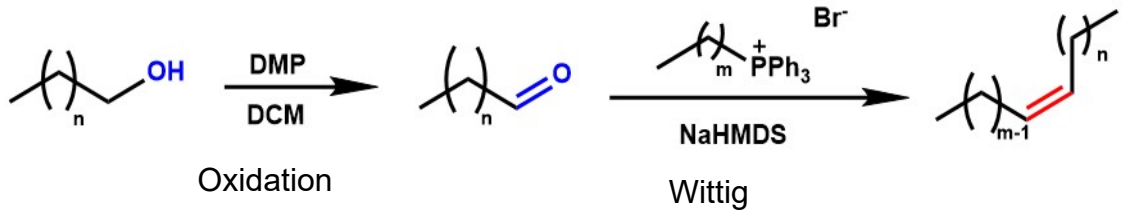

The first step was an oxidation reaction (Figure 2) where an alcohol group was oxidized into an aldehyde group using a hypervalent iodine compound, Dess-Martin periodinane. The carbonyl compound produced from this reaction was a starting material for the synthesis of *Z*-isomers of C_{25} and C_{27}.

Figure 2. Oxidation Reaction

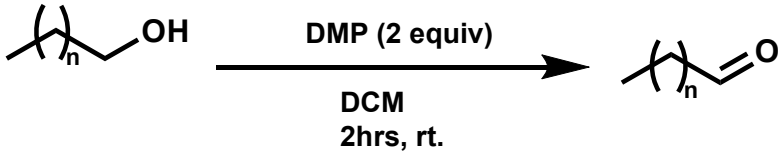

A general mechanism of the oxidation reaction, shown in Figure 3, involved alcohol group coordinating at the DMP iodine center. This led to the removal of one of the acetate ligands and diacetoxyalkoxyperiodinane was formed as an intermediate. The second acetate ligand in the iodine center deprotonated the α-hydrogen of the alcohol compound and formed a

C=O π bond. The carbonyl compound left the iodine center and kicked off another acetate ligand from the iodine center. A carbonyl compound was formed as product and acetic acid and iodinane as byproducts.

Figure 3. Mechanism of Oxidation Reaction using Dess-Martin Periodinane as a Reagent.

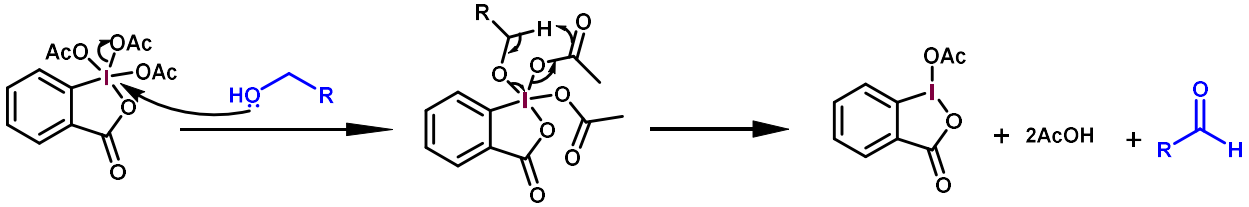

In order to prepare starting material for the hydrocarbon *Z*-alkenes, an alcohol group such as hexadecanol (**7**) was dissolved in dichloromethane and DMP was added while the solution was placed in ice bath. DMP can be explosive at high temperature, hence, DMP was added at low temperature around 0°C. The reaction was stirred for 2 hours and quenched with sodium bicarbonate and sodium thiosulfate for 10 minutes. Aqueous extraction was performed and concentrated in vacuo to yield hexadecanal (**8**) with a yield of 93%. The reaction was monitored with TLC and GC.

The oxidation reaction was repeated for heptadecanol (**4**), octadecanol (**1**), nonadecanol (**13**), and eicosanol (**10**) to get heptadecanal(**5**), octadecanal (**2**), nonadecanal (**14**), and finally eicosanal (**11**) with yields between 73% to 93%. The reactions were monitored with TLC and GC. Proton NMR was performed to verify compounds **2, 5, 8, 11, 14** was matched with the known spectral data.[18] The overall scheme of the oxidation reaction to prepare an aldehyde compounds are shown in Figure 4.

Figure 4. Reaction Scheme of Preparation of Aldehyde Compounds.

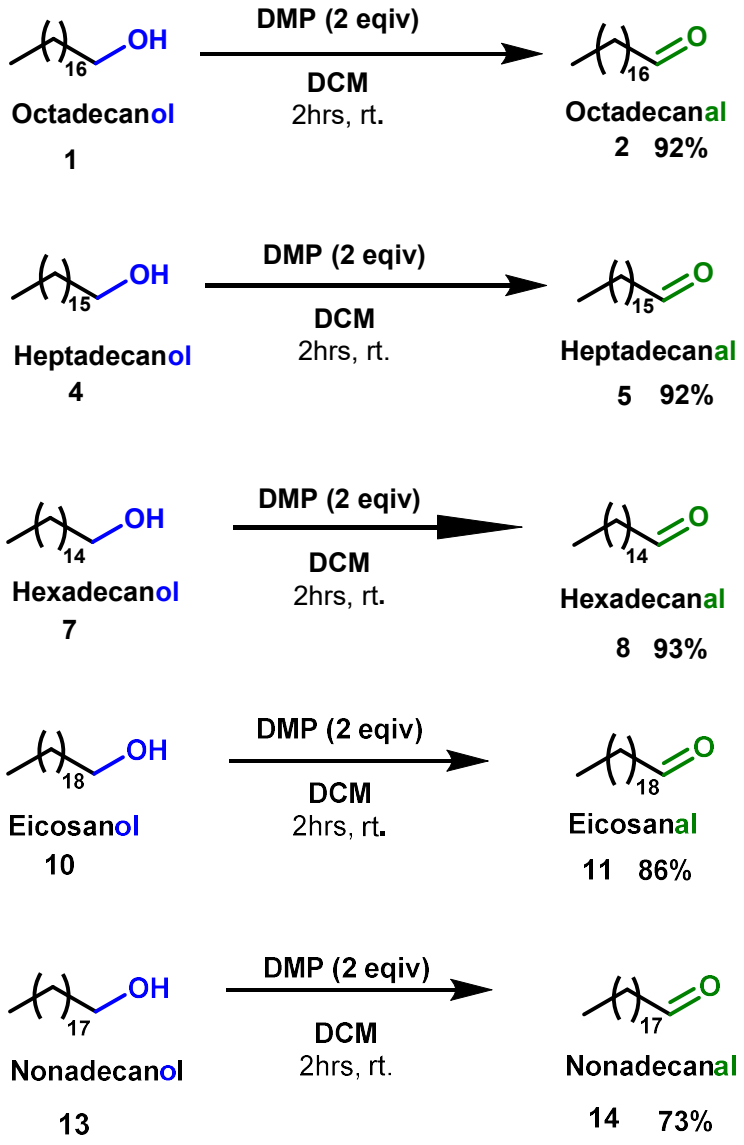

The second step of the synthesis of *Z*-isomers of C_{25} and C_{27} was a Wittig reaction (Figure 5). In this reaction, an aldehyde was reacted with the appropriate alkyl triphenyl phosphonium bromide and NaHMDS to yield a *Z*-alkene with a 25 or 27 carbon chain. The *Z*-alkene was synthesized in carbon positions 7, 8, and 9 for both C_{25} and C_{27}.

Figure 5. Wittig Reaction.

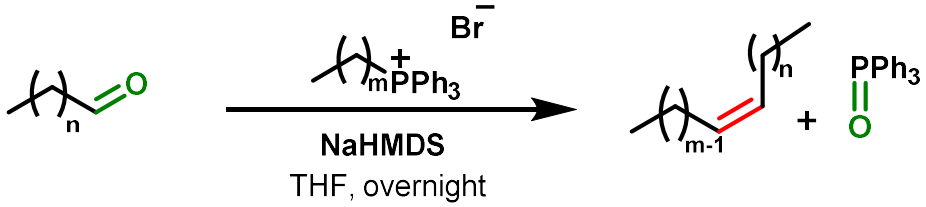

A general mechanism, shown in Figure 6, involved a nucleophilic attack of the negatively charged carbon atom of the ylide on the carbonyl group to obtain oxaphosphatane. The phosphorous intermediate immediately decomposed to yield the alkene and triphenylphosphine oxide. It was a concerted step because bonds break and formed simultaneously.[30] The driving force of the Wittig reaction was the formation of a very strong phosphorus-oxygen pi bond.

Figure 6. Mechanism of Wittig Reaction.

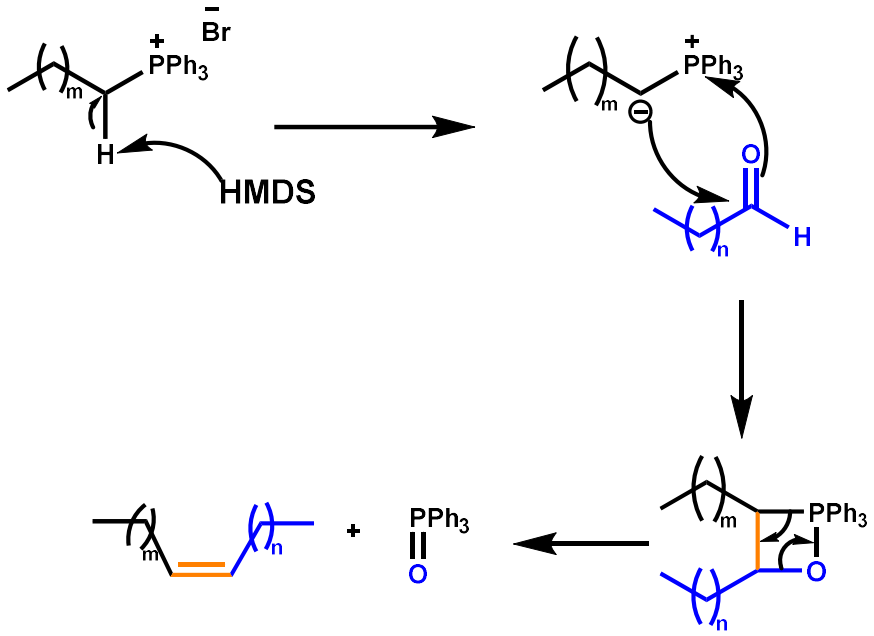

To synthesize the *Z*-9 C_{25}, 1 equivalent of (nonyl)-triphenyl phosphonium bromide was dissolved in THF, followed by the addition of 1 equivalent of NaHMDS, and finally 1 equivalent of hexadecanal (**8**) was added dropwise while placing the solution in an ice bath with brine. Brine was added to the ice bath to lower the temperature of the ice bath to less than 0°C. The

reaction was stirred overnight while letting the temperature to rise to room temperature. Once the reaction was completed, the mixture was concentrated in vacuo and purified through silica gel column chromatography. *Z*-9 C_{25} (**9**) was obtained with a yield of 80% (Figure 7). The resulting compound was a colorless oil and obtained with purity greater than 95% obtained through GC. ^{1}H and ^{13}C were performed to verify the compound.

Figure 7. Wittig Reaction for Synthesis of Z9-C25.

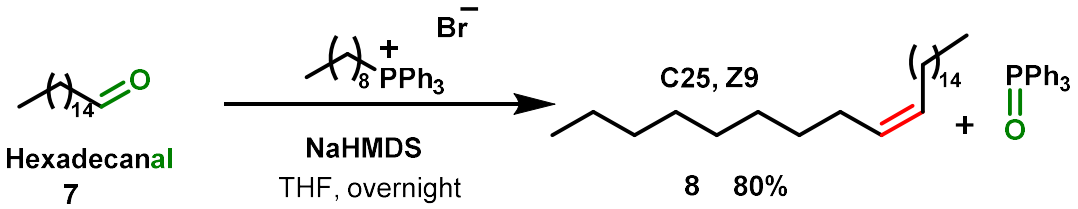

Similar methods were used to prepare other isomers of C_{25} and C_{27}. *Z*-7 C_{25} was formed with octadecanal (**2**) as a starting material implementing wittig reaction with 38% yield. *Z*-8 C_{25}, *Z*-7 C_{27}, *Z*-8 C_{27}, and *Z*-9 C_{27} were prepared with heptadecanal(**5**), eicosanal (**11**), nonadecanal (**14**), and octadecanal (**2**) respectively with yields between 42% to 88% (Figure 8). The purity of all the compounds were greater than 95% obtained through GC. ^{1}H and ^{13}C were performed to verify the synthesized compounds.

Figure 8. Wittig Reactions for Synthesis of *Z*-7 C25, *Z*-8 C25, *Z*-7 C27, *Z*-8 C27, and *Z*-9 C27, respectively.

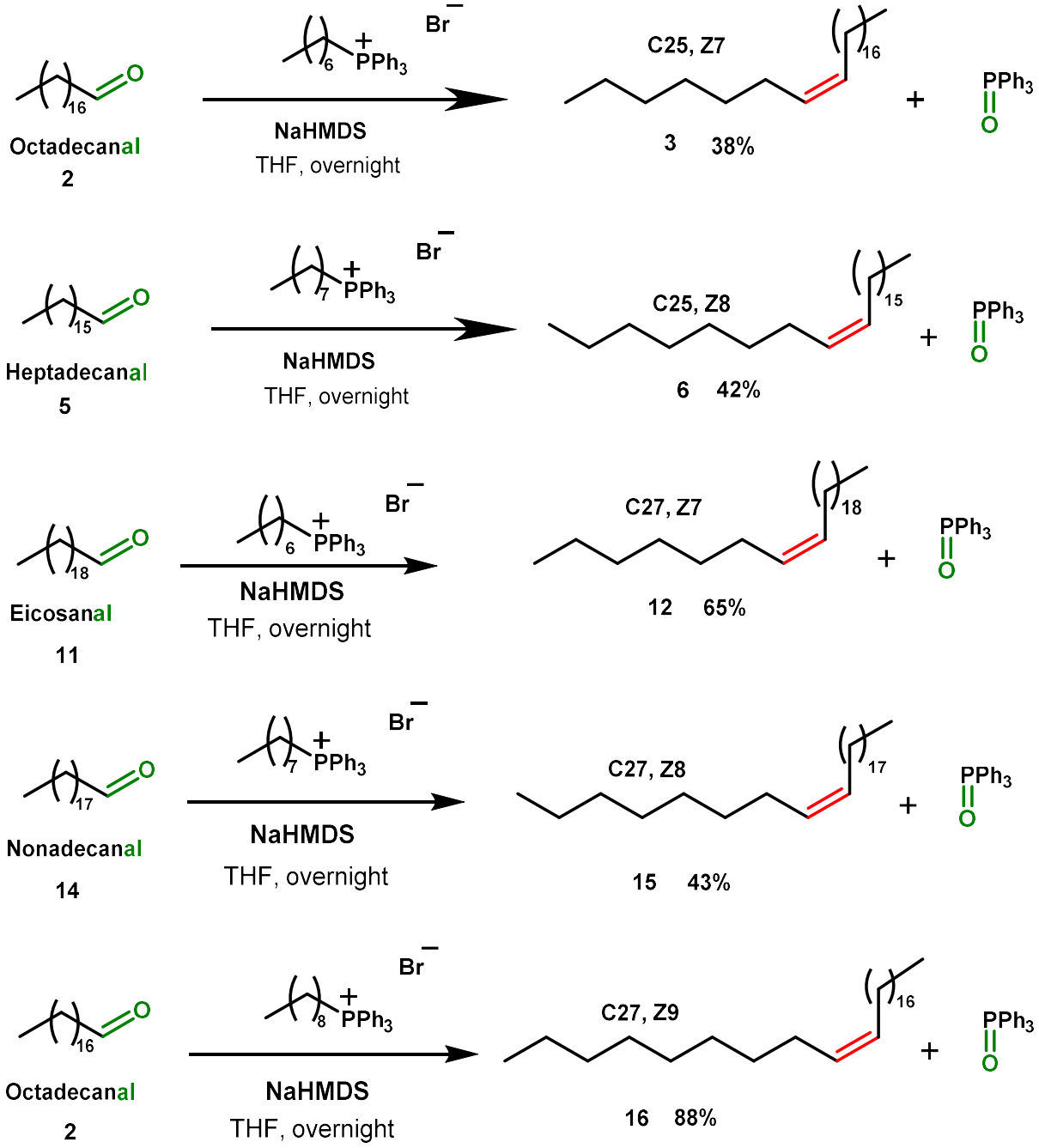

Initially, the synthesis of the alkenes was performed using 1 equivalent of aldehyde starting materials, 2 equivalents of NaHMDS and 2 equivalents of alkyl-triphenyl phosphonium bromides. The reactions were monitored by GC and silica gel column chromatography was used to purify the products. GC was obtained for some of the fractions which showed two peaks at

different retention times (Figure 9). The peak at 17.5 correlated to compound **9** (*Z*-9 C_{25}) while the peak at 13.9 correlated to the formation of byproduct. The byproduct that was formed during the reaction caused challenges in the purification of the compounds because when the products were purified through silica gel column chromatography, the byproducts eluted along with the desired products. All fractions that contained the desired product also contained the byproduct at varying percentage (1%-40%). For instance, during the purification of compound **9**, the GC showed that the first two-three fractions contained about 5% of byproduct peak and 95% product peak, while the rest of the fractions contained more than 5% of byproduct peaks.

Figure 9. GC Result to Show Formation of Byproduct (13.921) and Product (17.845) Peaks for Compound 9.

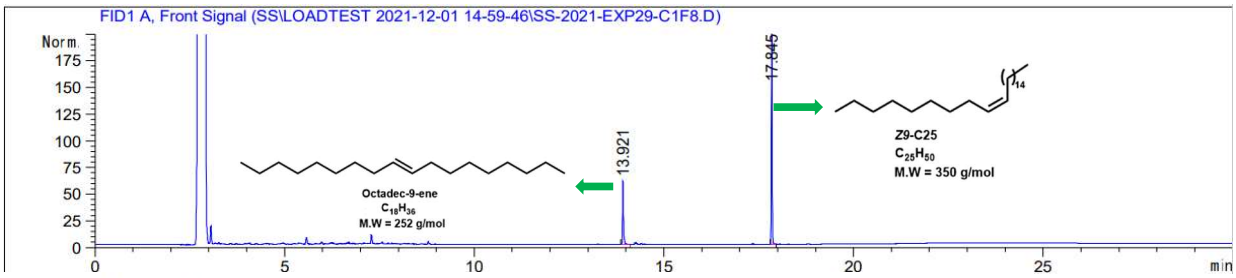

Signal 1: FID1 A, Front Signal

Peak #	RetTime [min]	Type	Width [min]	Area [pA*s]	Height [pA]	Area %
1	13.921	BB	0.0245	99.85742	59.64120	23.41471
2	17.845	BB	0.0223	326.61557	234.25876	76.58529

In order to determine the identity of the byproduct, GCMS was obtained. Based on the result from GCMS, it was hypothesized that the excess alkyl-triphenyl phosphonium bromide reacted with itself to produce a dimer. For instance, nonyl-triphenyl phosphonium bromide was used in the synthesis of *Z*-9 C_{25} (compound **9**), which reacted with itself to produce the dimerized byproduct (Figure 10). The mass shown in the GCMS correlated with the molecular weight of the dimerized byproduct of compound **9**.

Figure 10. EI Spectra of the Byproduct of Compound 9.

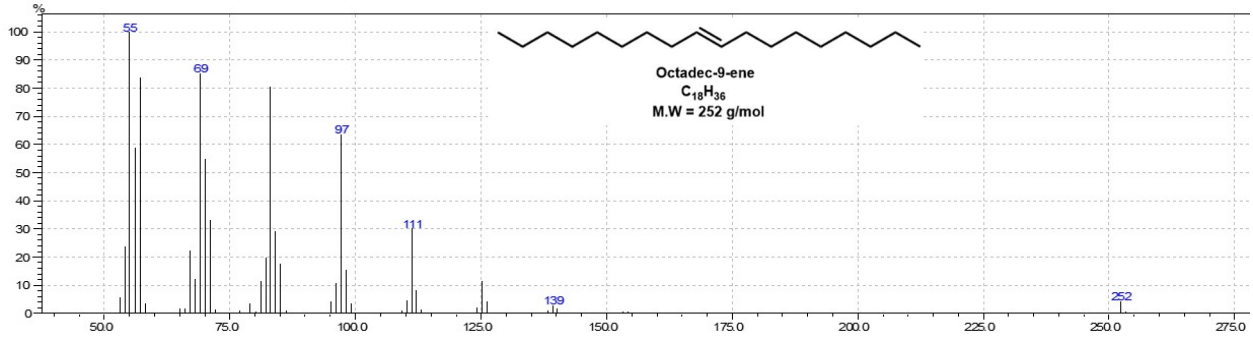

A putative mechanism is shown in Figure 11 for the byproduct of compound **9.** The first step would be formation of carbanion on 1-nonyl-triphenyl phosphonium bromide. The second step would be nucleophilic substitution of another 1-nonyl-triphenyl phosphonium bromide followed by removal of the triphenyl phosphonium bromide from the other hydrocarbon. The last step would be deprotonation, followed by formation of double bond, then removal of the triphenyl phosphonium bromide to yield the dimerized alkene byproduct.

Figure 11. Putative Mechanism for Dimerization of Nonyl-triphenyl Phosphonium Bromide.

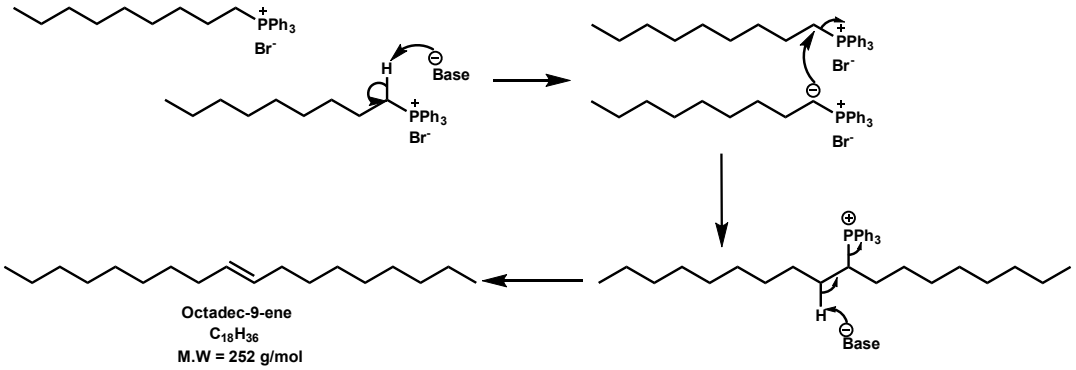

The GCMS was also obtained for other compounds and the results showed the formation of dimers which depended on the alkyl-triphenyl phosphonium bromide used. The mass spectra correlated with the molecular weight of the dimerized alkene form of alkyl-triphenyl phosphonium bromide for the byproducts of all six compounds. For both C_{25} and C_{27}, same

byproducts were formed for the same alkyl-triphenyl phosphonium bromide used. For instance, the byproduct for *Z*-9 C_{25} and *Z*-9 C_{27} were identical due to the use of nonyl-triphenyl phosphonium bromide in the reaction.

The challenges in the purification due to the formation of byproducts was improved by changing the equivalents of the alkyl-triphenyl phosphonium bromide as well as NaHMDS. Instead of using 2 equivalents of triphenyl phosphonium bromide and 2 equivalents of NaHMDS, the reaction was performed in 1 equivalent of both. The byproduct was still formed, however, with 1 equivalent of alkyl-triphenyl phosphonium bromide, it was formed in a lesser amount. Many fractions contained 87-99% desired product and only 1-13% of byproducts. Purity of greater than 95% was obtained for all six compounds are shown in Table 1. The summary of the synthesis with their corresponding percent yields are also shown in Table 1.

Table 1. Summary of Alkene Synthesis with Amounts Prepared Purity of Compounds and Percent Yields.

Compound	*Z*7-C25	*Z8*-C25	*Z9*-C25	*Z7*-C27	*Z8*-C27	*Z9*-C27
Amount (mg)	525	670	510	750	610	1000
Purity (%)	97	96	97	98	97	96
Yield (%)	38	42	80	65	43	88

Future Work and Conclusion

The goal of this project was to synthesize the six monoalkenes, *Z*-7 C_{25}, *Z*-8 C_{25}, *Z*-9 C_{25}, *Z*-7 C_{27}, *Z*-8 C_{27}, and *Z*-9 C_{27}, with purity greater than 95%. These compounds will be used in field testing for biological activity. Similar to previously identified hygiene-inducing compounds, *Z*-6 C_{15}, *Z*-8 C_{17}, *Z*-8 C_{31}, and *Z*-10 C_{33}, these compounds can be tested for their

ability to trigger a honeybee hygienic response. A significant negative correlation between colony hygienic response to a compound and colony *Varroa* infestation would indicate that the compound is a good candidate for incorporation into a tool to measure honeybee colony pest and disease resistance. Thus, this work has the potential for development of improved control of mites and facilitate selective breeding of *Varroa*-resistant honeybees.

In terms of the techniques used in the synthesis of the monoalkenes, improvements in the yields of the compounds will be targeted in the near future. The yields can be improved by using dry and freshly bought NaHMDS because NaHMDS could have been wet and caused an incomplete reaction. The identity of the byproduct should also be confirmed in the future works by attempting to isolate the byproduct from the product and obtaining the NMR data.

CHAPTER III: HETEROCYCLE FORMATION INTRODUCTION

Stereoisomers

Compounds that differ in the spatial arrangement of atoms and have same structural formulas are known to be stereoisomers. Stereoisomers can be further categorized as conformational isomers and configurational isomers. The conformational isomers are stereoisomers produced by rotation about σ bonds and can be interconverted. Configurational isomers are stereoisomers that do not interconvert without breaking bonds and have different configurations. An interesting type of isomer are the mirror-image stereoisomers which is a non-superimposable set of two molecules that are mirror images of one another. The existence of these molecules is determined by the concept of chirality.

Chirality is derived from Greek, *kheir*, "hand" which is a chiral object. The left and right hands are mirror images of one another, but they are non-superimposable. A left-hand glove cannot fit in the right-hand glove because hands do not have a mirror plane of symmetry. Chiral molecules can have more than one chiral centers. A chiral center is when an atom in a molecule is bonded to four different chemical species. An example of chiral molecules can be seen in Figure 12. Molecule A is a tetrahedral carbon with four different substituents H, Br, Cl, and F and molecule B is a mirror image of A. Molecule A lines up with molecule B at every point through a mirror. When molecule A is flipped 180° in an attempt to superimpose to molecule B, it cannot be superimposed, as shown in Figure 13. Because A is not superimposable on its mirror image, B, both molecules are chiral.

Figure 12. Bromochlorofluoromethane Chiral Molecule.

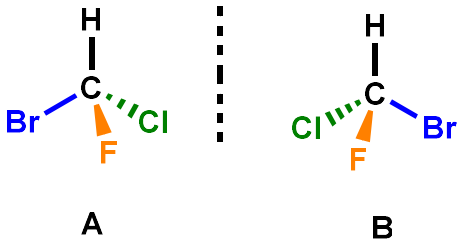

Figure 13. Rotation of Molecule A about 180° with Attempt to Superimpose Molecules A and B.

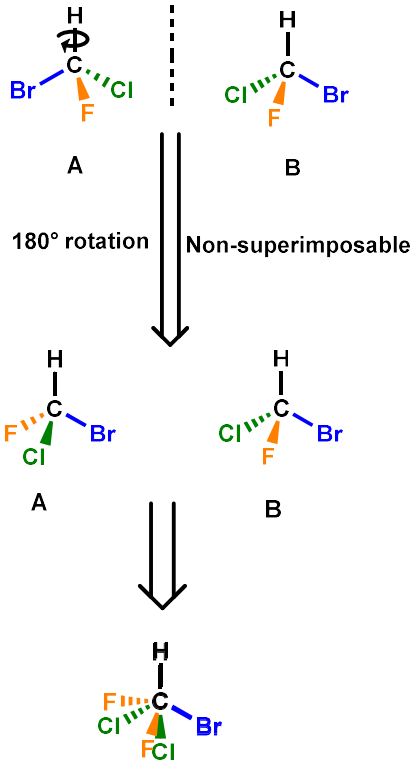

Molecules A and B are specific type of stereoisomers called enantiomers. They are mirror images of one another and do not superimpose. Enantiomers have identical physical properties such as boiling point, melting points and densities.

Indole-Containing Compounds

The indole moiety is present in many natural alkaloids that display a wide range of biological activities as well as in pharmaceutical agents.[19] Indole is a bicyclic, aromatic organic compound with a formula C_8H_7N. It contains a six-membered benzene ring that is fused to a

five-membered pyrrole ring and has 10 π-electrons that participates in aromaticity. Indole was first isolated in 1866 [20] and Fischer indole synthesis is the most popular method to prepare indole rings. It is prepared from aryl hydrazine and aldehyde or ketone by treatment with acid catalyst [20] (Figure 14). Indole undergoes electrophilic aromatic substitution at C-3 position, the most reactive site of indole. Reactions involving indoles include aromatic halogenation, aromatic sulfonation, aromatic nitration, and Friedel-Crafts alkylation reactions.[21]

Figure 14. Fischer Indole Synthesis Reaction.

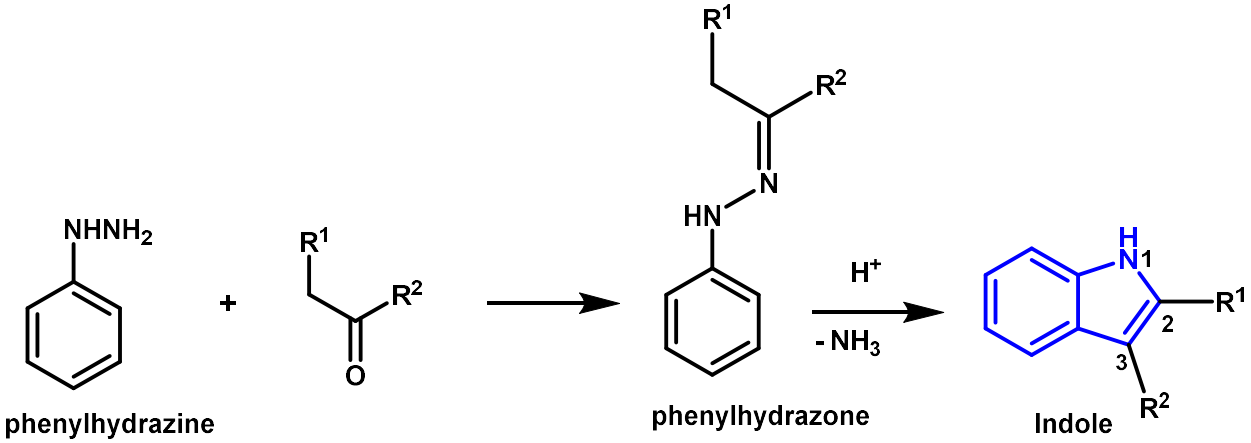

L-tryptophan is an amino acid that contains an indole moiety (Figure 15) and is essential for making proteins. It can be found naturally in red meat, poultry, eggs, and dairy. The amino acid cannot be produced by the body and must be consumed from diet. Another example of indole containing compounds are ergot alkaloids. The four main types of ergot alkaloids are lysergic acids, lysergic acid amides, clavines and ergopeptides (Figure 15). Ergot alkaloids are produced by numerous groups of fungi species of the genus *Claviceps,* typically found in tropical areas affecting crops such as cereals and grass.[22] Ergot alkaloids are used in treatment of migraines, induction of childbirth, and control of postpartum bleeding.[22]

Figure 15. L-Tryptophan and Four Ergot Alkaloid Types- D-Lysergic Acid, Lysergic Acid Amide, Argoclavine, and Ergotamine.

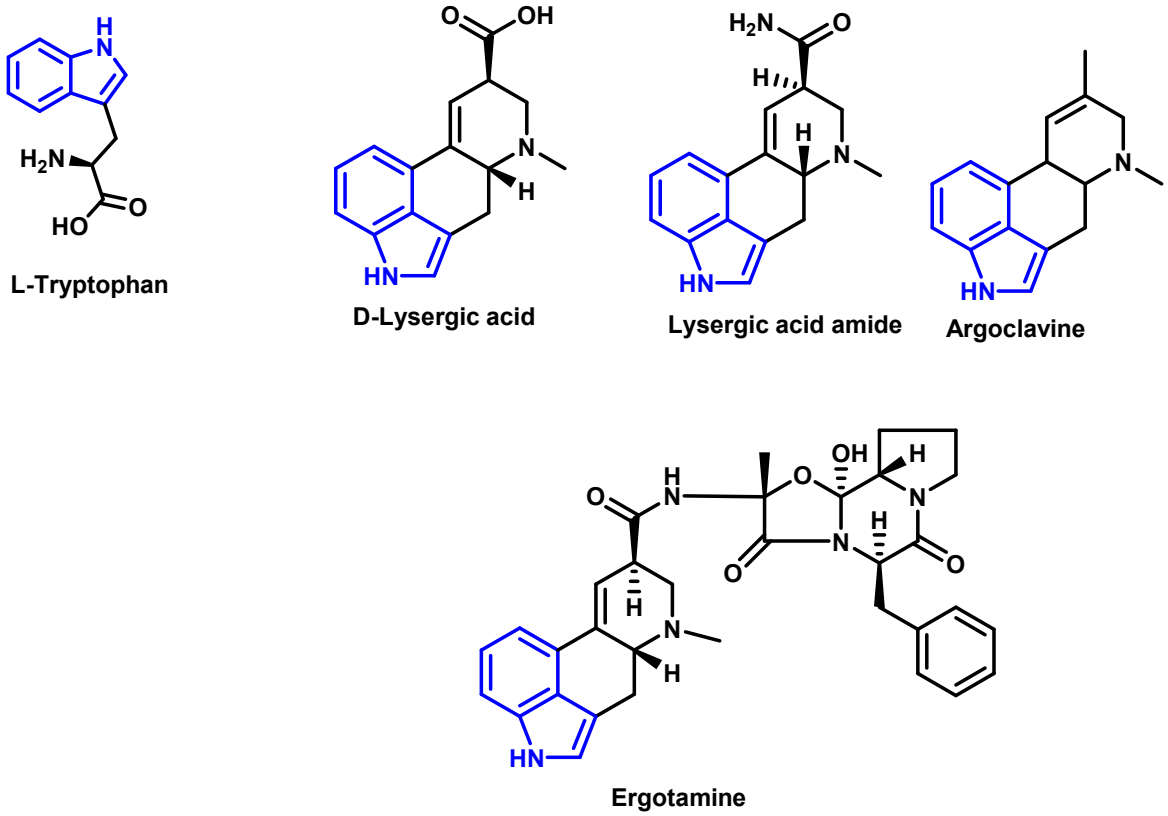

Brønsted Acid Catalysts

A Brønsted acid is a chemical species that donate protons. Some examples of Brønsted acids are *p*-toluenesulfonic acid, methylsulfonic acid, and 3,3'-bis (2,4,6- triisopropylphenyl)-1,1'binaphthyl-2,2'-dihydrogen phosphate (TRIP) (Figure 16). Acid catalyzed reactions with p-toluenesulfonic acid and methanesulonic acid, achiral Brønsted acids, produce racemic mixtures. Hence, to perform a stereoselective reactions, use of a chiral acid such as phosphoric acid TRIP catalyst is essential.

Figure 16. p-Toluenesulfonic Acid, Methanesulfonic Acid, and (R)-TRIP Catalyst.

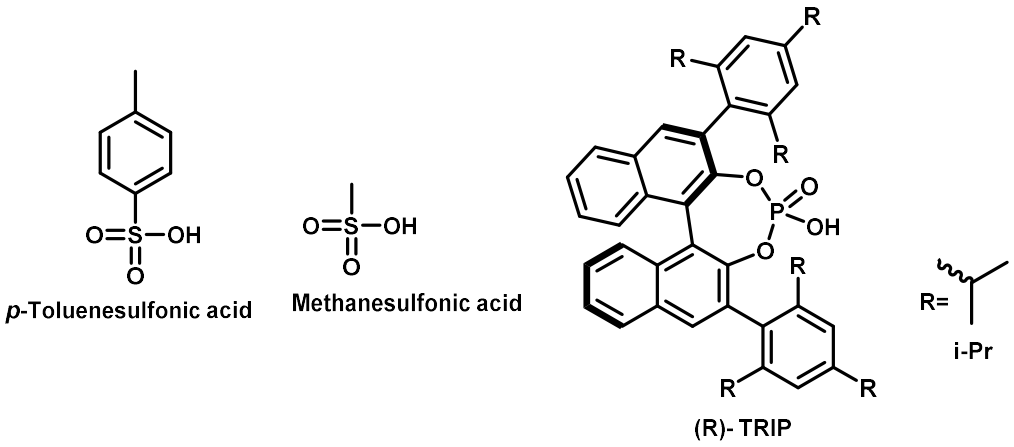

TRIP catalyst has key characteristics that allows it to be an ideal catalyst for producing enantioenriched heterocyclic building blocks (Figure 17). First, the hydroxyl hydrogen of the phosphoryl group in TRIP can act as Brønsted acid and the phosphoryl oxygen can act as a Brønsted base for hydrogen bonding interactions with the malonic ester. These interactions produce a complex between the chiral phosphoric acid and the malonic ester.[23] Cyclization is promoted through the proximity of the electrophilic carbon atom of the ester group and the nucleophilic oxygen atom of the hydroxyl group of the malonic acid derivatives.[23] Second, for the cyclization process, the 3,3' aryl groups of the TRIP catalyst act as stereo-controlling groups.[23] TRIP catalyst only produces certain enantiomers of malonic ester derivatives, and it provides steric hinderance for formation of other enantiomers. Lastly, the 1,1'-bi-2- naphthol (BINOL) backbone has an R or S orientation that can control the directionality of the aryl group and influences the reactivity of TRIP catalyst.[23]

Figure 17. Proposed Activation Complex Between (R)-TRIP Catalyst and Malonic Ester.

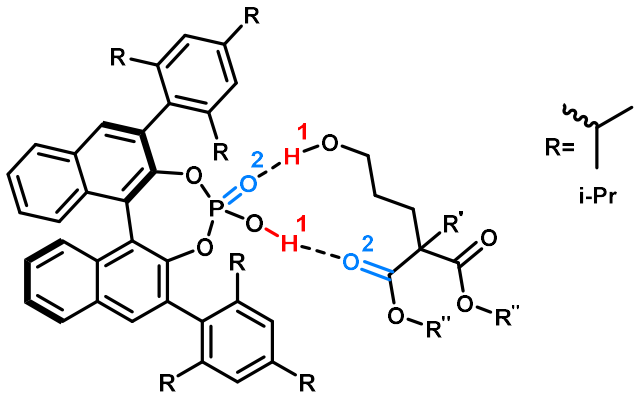

(R)- TRIP 1 = Brønsted acid

2= Brønsted base

Previous Work of Dr. Petersen Group

Previously, desymmertrization reactions were used to produce enantioenriched lactone derivatives with the use of malonic esters. This was a novel asymmetric technique developed by Dr. Jennifer Wilent of Dr. Petersen group. The main focus of her work was on the synthesis of γ-lactone,[24] which was achieved with high yields (Figure 18) and enantioselectivities.

Figure 18. Work Accomplished by Dr. Jennifer Wilent.

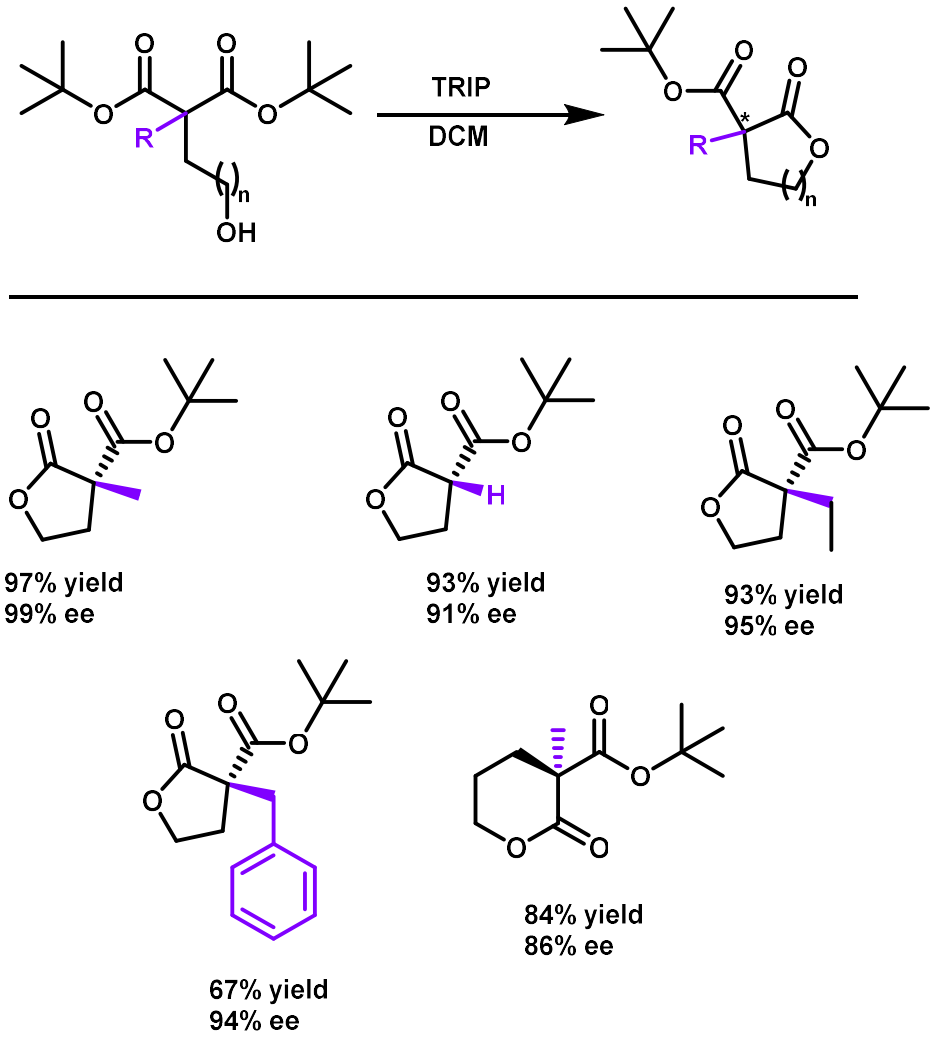

Furthermore, Dr. Wilent's work was expanded by Dr. Amber Kelley and graduate student Rhashanda Haywood. They worked with coumarin derivatives which were produced from cyclic substrates from desymmetrization reactions. The 3,4-dihydrocoumarin derivatives were produced in moderate to high yields[25] (Figure 19). Based on the results of Dr. Kelley, the secondary alkyl groups did not contribute significantly to the decrease of ee as the steric size increased. Additionally, the quaternary carbon centers were produced in high yield and ee.

Figure 19. : Work Accomplished by Dr. Amber Kelly.

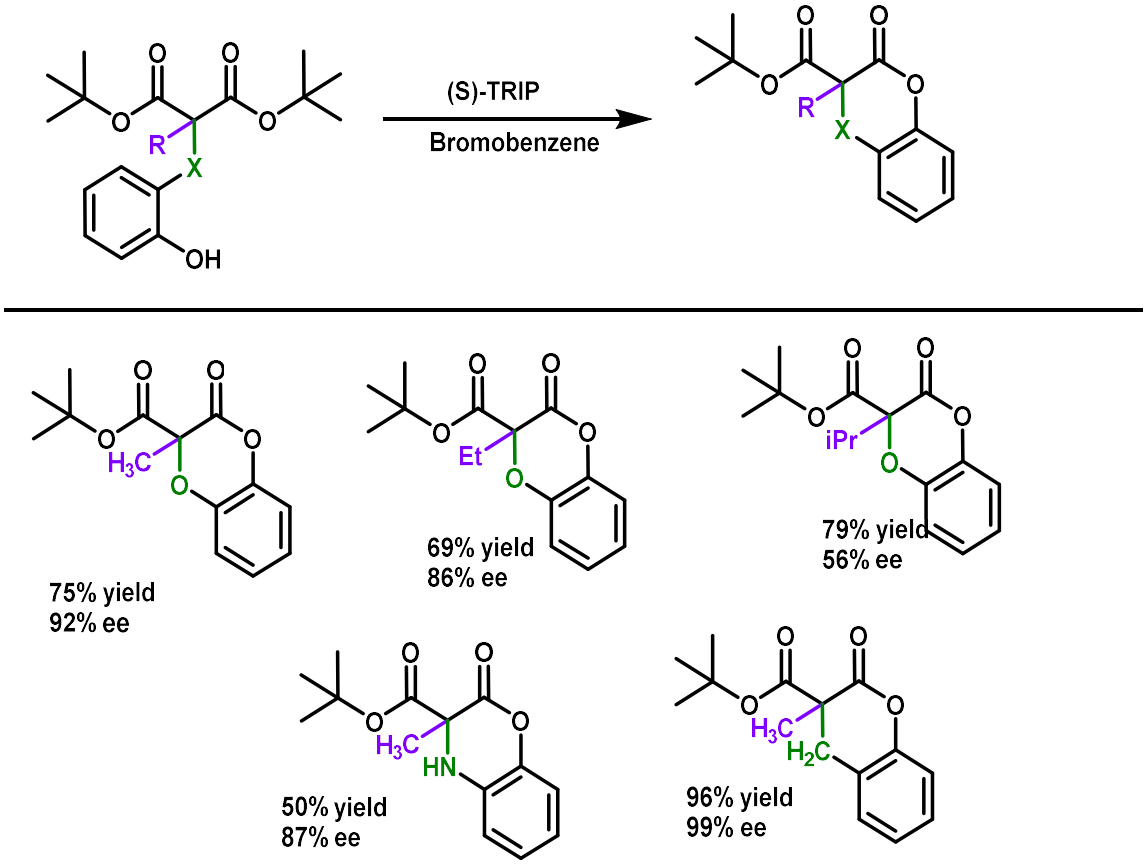

Following on the footstep of Dr. Wilent's work, Dr. Petersen group is focused on preparing alternative heterocyclic small molecules. This research is focused on formation of carbon-carbon bonds which is potentially novel and chemically significant. The proposed enantioselective synthesis of a heterocycle is performed through a series of synthetic steps, starting with commercially available indole moiety and malonic ester.

CHAPTER IV: CARBON-CARBON BOND FORMATION PRODUCING ENANTIOSELECTIVE HETEROCYCLE

Present Works

With information provided by previous researchers from Dr. Petersen's group, this research provided an expansion of stereoselective formation of heterocycles through desymmetrization of a malonic ester derivative. A goal of this project was to synthesize compound **20**, which will then be used to form a novel carbon-carbon bond (compound **21**) using a Brønsted acid. The ultimate goal of this research, however, was to form an additional fused ring on the indole substituent, transforming a bicyclic, compound **20** into a tri-cyclic, compound **21**, in addition to forming a new chiral center on the newly synthesized compound **21**.

Compound **20** was not commercially available and in order to synthesize the compound, a Knoevenagel condensation followed by hydrogenation reactions was implemented. The Knoevenagel condensation reaction involved reacting diethyl malonate and indole-4-carboxyaldehyde to form compound **19**. Compound **19** was reacted with palladium on carbon (Pd/C) and hydrogen gas to produce compound **20**. Compound **20** was alkylated and cyclized via desymmetrization where a new carbon-carbon bond is formed as a product. The overall reaction schemes are shown in Figure 22.

Figure 20. Proposed Synthetic Pathway for Formation of Compound 21.

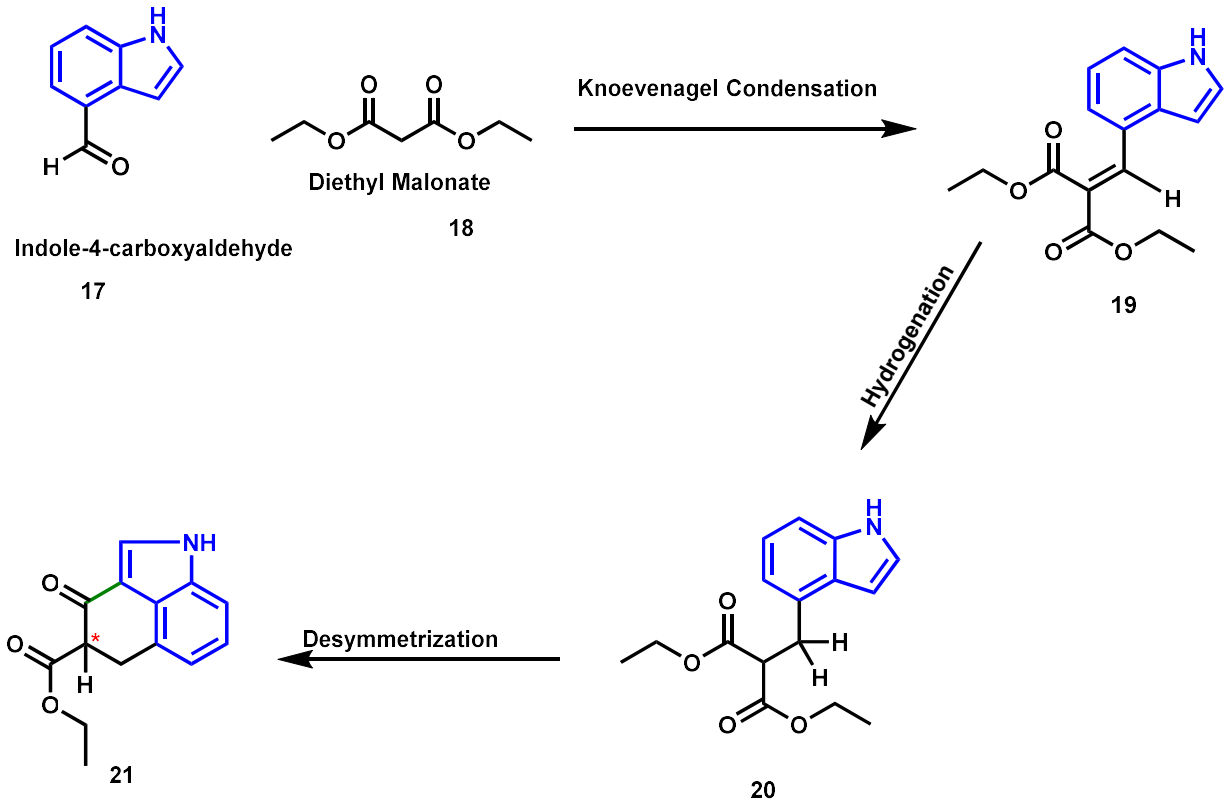

Note: Red Asterisk Denotes Desired Enantioenriched Carbon and Green Bond Denotes Carbon-Carbon Bond Formation.

The first step as mentioned previously in the synthesis of the novel enantioselective heterocycle was Knoevenagel condensation (Figure 21). This reaction involved a nucleophilic addition of a malonic ester compound into a carbonyl group in the presence of a base followed by dehydration of water molecule. The product formed from Knoevenagel condensation was α,β-unsaturated ketone. Knoevenagel condensation reaction was a variant of aldol condensation. The general mechanism, shown in Figure 24, of Knoevenagel condensation began with an acid/base reaction between malonic acid and piperidine. The piperidine deprotonated the diketone to give a carbanion and forms resonance stabilized anion or enolate. The enolate acted as a nucleophile and attached to the carbonyl of the aldehyde. Tetrahedral intermediate that was formed was then

protonated by the piperidinium forming an aldol. The aldol then performed a dehydration reaction to form a was α,β-unsaturated ketone.

Figure 21. Knoevenagel Condensation Reaction.

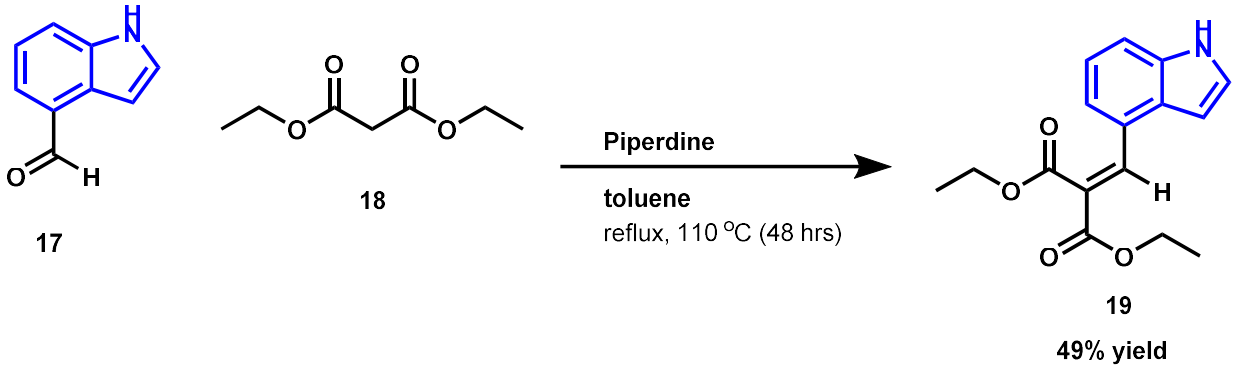

Figure 22. Proposed Mechanism of Knoevenagel Condensation.

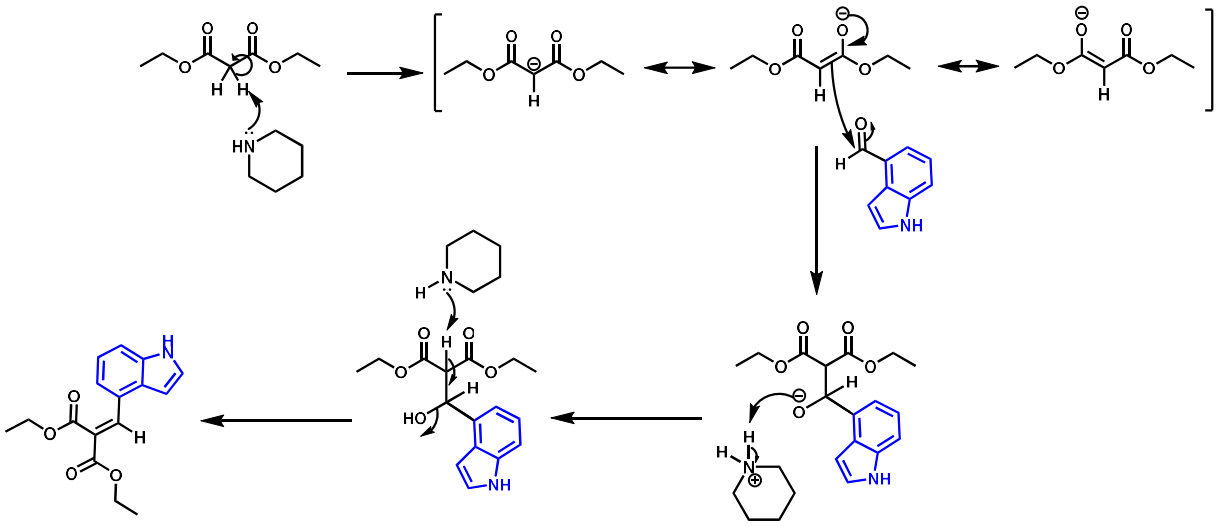

Knoevenagel condensation began with reacting an indole-4-carboxyladehyde and diethyl malonate in the presence of piperidine and heat. The temperature used for the reaction depended on the boiling point of the solvent, in this reaction, toluene. Once the materials were added, the reaction was refluxed for 48 hrs and concentrated in vacuo. The resulting compound **19**, was produced with a yield of 49%. The reaction was monitored by TLC and NMR.

Once compound **19** was produced, the second step in the process was to perform a hydrogenation reaction in order to reduce the double bond formed during Knoevenagel condensation. The central double bond was removed to ensure the presence of sigma bond to allow flexibility for the next step in the synthesis (cyclization). Hydrogenation reaction was performed by adding compound **19** with palladium on carbon (Pd/C) and hydrogen gas (Figure 23). The reaction was stirred for 24 hrs at room temperature and compound **20** was produced with a 60% yield.

Figure 23. Hydrogenation Reaction of Compound 20.

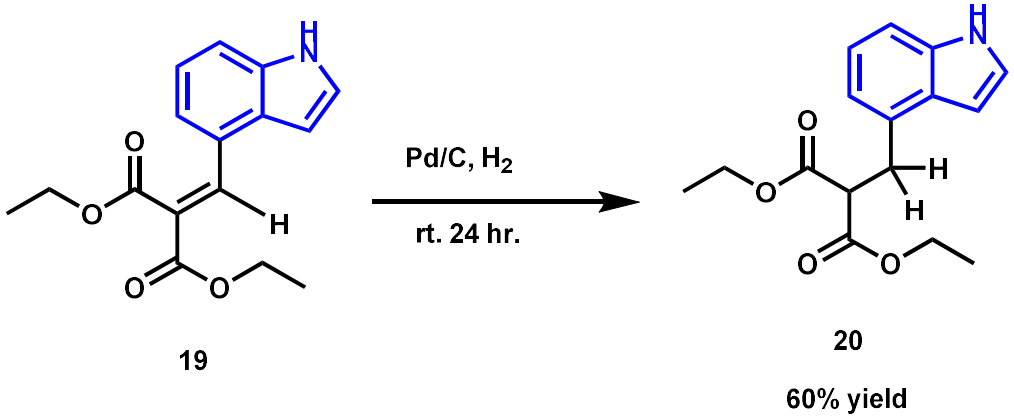

After compound **20** has been produced, the final step in this process was to attempt to cyclize compound **20** with Brønsted acid catalyst and determine if a carbon-carbon bond was formed (Figure 24). To attempt to perform cyclization reaction, compound **20** was reacted with p-toluenesulfonic acid and heated at 80 °C. However, cyclized product was not observed (Figure 25).

Figure 24. Proposed Desymmetrization Reaction of Compound 20 in the Presence of Brønsted Acid.

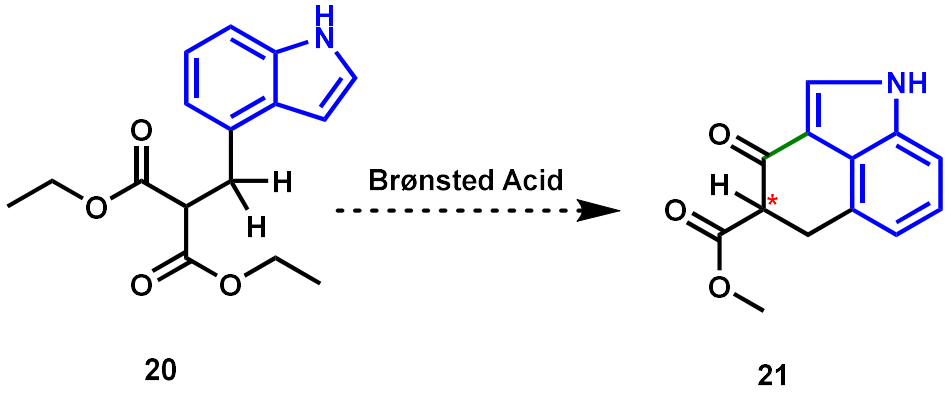

Figure 25. Failed Attempt to Desymmetrize Compound 20 in Presence of p-Toluenesulfonic Acid.

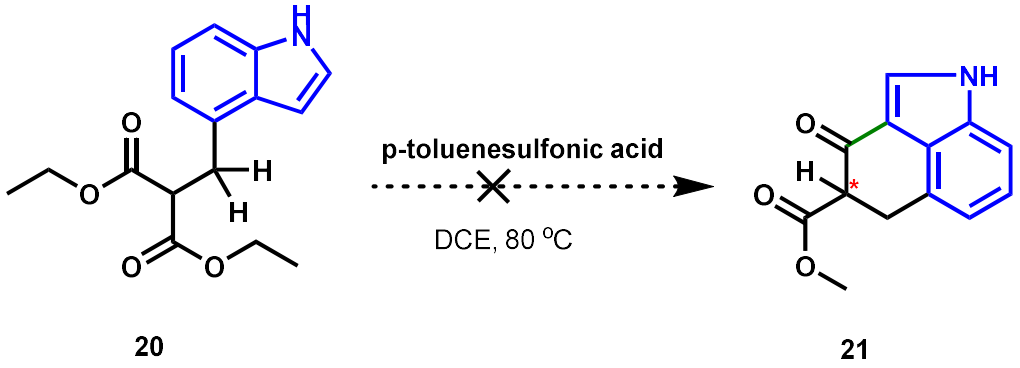

Future Works and Conclusion

The goal of the project was to produce an enantioenriched heterocycle with a desymmetrization reaction to form a novel carbon-carbon bond. The cyclization process was deemed unsuccessful and did not yield a desired product (compound **21**). Based on the knowledge from previous work in Dr. Petersen's group, desymmetrization reactions are dependent on temperature and time, therefore, reactions should be performed with different reaction conditions to allow the reaction to go to completion. If the reaction is to be repeated, changes in solvent to obtain different temperatures could improve the reaction outcome. Another approach would be to use different Brønsted acid catalysts to attempt to cyclize. The next step in

the project after successfully synthesizing compound **21** would be to use TRIP catalyst to obtain an enantioenriched heterocycle through cyclization.

CHAPTER V: EXPERIMENTAL PROCEDURES AND METHODS

General Information

All reactions were performed with dried solvents in an oven dried glassware under an argon atmosphere. Solvents and reagents were obtained from commercial sources and used without additional purification. Purification was performed using flash grade silica gel (particle size: 40-63 μm, 230 × 400 mesh). The reactions were monitored by TLC using silica G F254 precoated plates. The ^{1}H and ^{13}C NMR spectra were recorded on JOEL 400 MHz spectrometer. The solvent used to record the NMR was CDCl3 at room temperature. Coupling constants, *J*, are reported in hertz (Hz) and chemical shifts (δ) are reported in ppm. Multiplicities are listed as single (s), doublet (d), triplet (t), quartet (q), and multiplet (m). GC-MS with single quadrupole mass analyzer (QP2010S, Shimadzu) equipped with electron impact ionization was used to obtain EI mass spectra with a scan range 40 to 650m/z. following methods obtained from Wagoner et.al. (2019).[9]

Synthesis of Octadecanal (2)

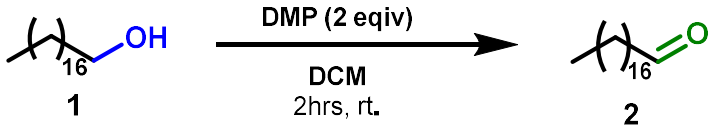

An oven dried 50-mL round bottom flask was obtained and equipped with magnetic stir bar and argon balloon. Octadecanol (**1**) (1.5 g, 5.5 mmol,) was added to the flask along with dry dichloromethane (40 mL). The mixture was stirred at room temperature until octadecanol (**1**) was dissolved. Dess Martin periodinane (4.7 g, 11.1 mmol) was added to the flask in ice bath and stirred for 2 hrs. The mixture was stirred with saturated sodium bicarbonate and sodium thiosulfate (1:1 v/v; 20 mL) for 10 minutes. The mixture was then extracted with ethyl acetate

(3× 20 mL). The organic layers were combined, dried with $MgSO_4$, filtered, and concentrated in vacuo. The mixture was purified by silica gel column chromatography (5% ethyl acetate/hexane) to obtain octadecanal (**2**) (1.3 g, 92% yield) as a white solid (m.p =38 °C).[26]

^{1}H NMR (400 MHz, Chloroform-d) δ 9.74 (s, 1H), 2.40 (t, *J* = 7.5 Hz, 2H), 1.55-1.68 (m, 2H), 1.17-1.39 (m, 28H), 0.86 (t, *J* =7.0 Hz, 3H).

Synthesis of Heptadecanal (5)

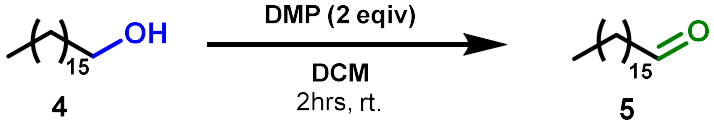

An oven dried 50-mL round bottom flask was obtained and equipped with magnetic stir bar and argon balloon. Heptadecanol (**4)** (1.5 g, 5.0 mmol,) was added to the flask along with dry dichloromethane (40 mL). The mixture was stirred at room temperature until heptadecanol (**4)** was dissolved. Dess Martin Periodinane (4.9 g, 10.0 mmol) was added to the flask in ice bath and stirred for 2 hrs. The mixture was stirred with saturated sodium bicarbonate and sodium thiosulfate (1:1 v/v; 20 mL) for 10 minutes. The mixture was then extracted with ethyl acetate (3*20 mL). The organic layers were combined, dried with MgSO4, filtered, and concentrated in vacuo. The mixture was purified by silica gel column chromatography (5% ethyl acetate/hexane) to obtain the Heptadecanal (**5)** (1.2 g, 92% yield) as a white solid (m.p 36°C).[26]

^{1}H NMR (400 MHz, Chloroform-d) δ 9.73 (s, 1H), 2.40 (t, *J* = 7.5 Hz, 2H), 1.54-1.67 (m, 2H), 1.18-1.35 (m, 26H), 0.86 (t, *J* =7.0 Hz, 3H).

Synthesis of Hexadecanal (8)

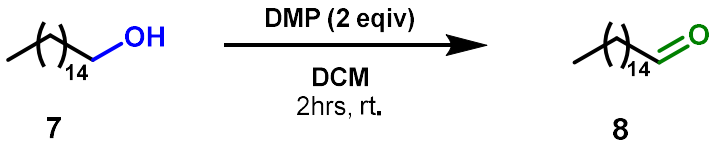

7 8

An oven dried 50-mL round bottom flask was obtained and equipped with magnetic stir bar and argon balloon. Hexadecanol (**7)** (402 mg, 2.0 mmol,) was added to the flask along with dry dichloromethane (20 mL). The mixture was stirred at room temperature until hexadecanol (**7)** was dissolved. Dess Martin Periodinane (1.7 g, 4.1 mmol) was added to the flask in ice bath and stirred for 2 hrs. The mixture was stirred with saturated sodium bicarbonate and sodium thiosulfate (1:1 v/v; 20 mL) for 10 minutes. The mixture was then extracted with ethyl acetate (3*15 mL). The organic layers were combined, dried with $MgSO_4$, filtered, and concentrated in vacuo. The mixture was purified by silica gel column chromatography (5% ethyl acetate/hexane) to obtain the hexadecanal (**8**) (372 mg, 93% yield) as a white solid (m.p 35 °C).[26]

^{1}H NMR (400 MHz, Chloroform-d) δ 9.74 (s, 1H), 2.42 (t, *J* = 7.5 Hz, 2H), 1.55-1.65 (m, 2H), 1.17-1.36 (m, 24H), 0.87 (t, *J* =7.0 Hz, 3H).

Synthesis of Eicosanal (11)

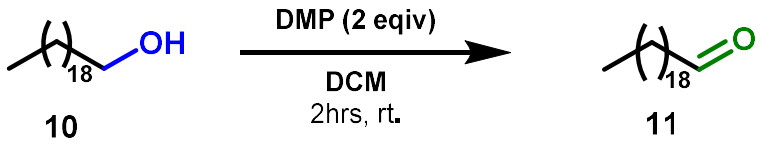

10 11

An oven dried 50-mL round bottom flask was obtained and equipped with magnetic stir bar and argon balloon. Eicosanol (**10)** (1.51 g, 5.0 mmol) was added to the flask along with dry dichloromethane (40 mL). The mixture was stirred at room temperature until eicosanol (**10)** was dissolved. Dess Martin Periodinane (4.25 mg, 10.0 mmol) was added to the flask in ice bath and stirred for 2 hrs. The mixture was stirred with saturated sodium bicarbonate and sodium

thiosulfate (1:1 v/v; 20 mL) for 10 minutes. The mixture was then extracted with ethyl acetate (3*20 mL). The organic layers were combined, dried with $MgSO_4$, filtered, and concentrated in vacuo. The mixture was purified by silica gel column chromatography (5% ethyl acetate/hexane) to obtain the eicosanal (**11**) (1.28 g, 86% yield) as a white solid (m.p 66°C).[26]

^{1}H NMR (400 MHz, Chloroform-d) δ 9.72 (s, 1H), 2.42 (t, *J* = 7.5 Hz, 2H), 1.53-1.67 (m, 2H), 1.16-1.37 (m, 32H), 0.85 (t, *J* =7.0 Hz, 3H).

Synthesis of Nonadecanal (14)

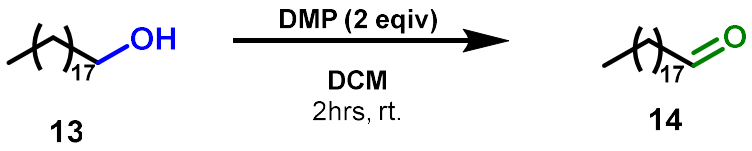

13 **14**

An oven dried 50-mL round bottom flask was obtained and equipped with magnetic stir bar and argon balloon. Nonadecanol (**13**) (1.5 g, 5.2 mmol,) was added to the flask along with dry dichloromethane (40 mL). The mixture was stirred at room temperature until nonadecanol (**13)** was dissolved. Dess Martin periodinane (4.4 g, 4.5 mmol) was added to the flask in ice bath and stirred for 2 hrs. The mixture was stirred with saturated sodium bicarbonate and sodium thiosulfate (1:1 v/v; 20 mL) for 10 minutes. The mixture was then extracted with ethyl acetate (3×20 mL). The organic layers were combined, dried with $MgSO_4$, filtered, and concentrated in vacuo. The mixture was purified by silica gel column chromatography (5% ethyl acetate/hexane) to obtain the nonadecanal (**14**) (1.1 g, 73% yield) as a white solid (m.p 44°C).[26]

^{1}H NMR (400 MHz, Chloroform-d) δ 9.70 (s, 1H), 2.42 (t, *J* = 7.5 Hz, 2H), 1.53-1.68 (m, 2H), 1.16-1.39 (m, 30H), 0.87 (t, *J* =7.0 Hz, 3H).

Synthesis of *Z*-7 C_{25} (3)

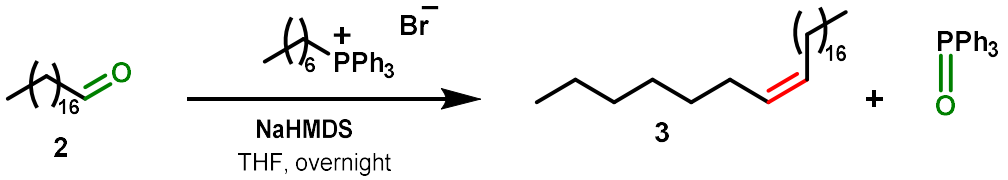

A 50 mL oven dried round bottom flask was equipped with magnetic stir bar and argon balloon. In the flask, (1-heptyl) triphenylphosphonium bromide (730 mg, 1.6 mmol) and THF (10 mL) were added and stirred. A solution of NaHMDS (2M in THF, 1.5 mL) was added and stirred. The solution is stirred at room temperature for 15 minutes then placed in an ice bath with brine to cool. Octadecanal (**2**) (403 mg, 1.5 mmol,) was dissolved in THF (10 mL) and the solution was added dropwise to the flask over 10 minutes. The mixture was warmed slowly and stirred overnight. The mixture was concentrated in vacuo and purified by silica gel column chromatography (100% hexane) to obtain *Z*-7 C_{25} (**3**) as colorless oil (199 mg, 38% yield).

^{1}H NMR (400 MHz, Chloroform-d) δ 5.33 (t, *J* = 7.4 Hz, 2H), 1.95-2.07 (m, 4H), 1.17-1.45 (m, 38H), 0.83-0.91 (m, 6H).

^{13}C NMR (101 MHz, Chloroform-d) δ 129.9, 32.0, 31.8, 29.9, 29.84, 29.80, 29.7, 29.6, 29.5, 29.4, 27.3, 22.8, 22.7, 14.2.

Synthesis of *Z*-8 C_{25} (6)

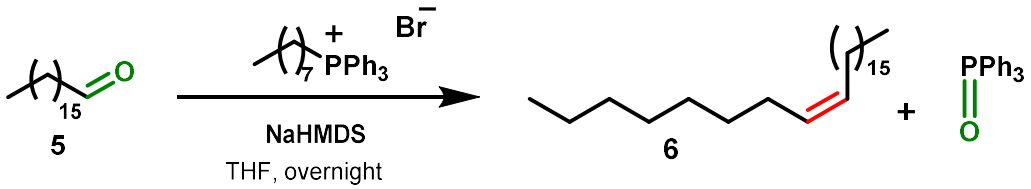

A 50 mL oven dried round bottom flask was equipped with magnetic stir bar and argon balloon. In the flask, (1-octyl) triphenylphosphonium bromide (1.8 g, 4.1 mmol) and THF (15 mL) were added and stirred. A solution of NaHMDS (2M in THF, 2.0 mL) was added and

stirred. The solution is stirred at room temperature for 15 minutes then placed in an ice bath with brine to cool. Heptadecanal (**5**) (520 mg, 2.0 mmol,) was dissolved in THF (5 mL) and the solution was added dropwise to the flask over 10 minutes. The mixture was warmed slowly and stirred overnight. The mixture was concentrated in vacuo and purified by silica gel column chromatography (100% hexane) to obtain *Z*-8 C_{25} (**6**) as colorless oil (299 mg, 42%).

^{1}H NMR (400 MHz, Chloroform-d) δ 5.34 (t, *J* = 7.4 Hz, 2H), 2.08-1.96 (m, 4H), 1.46-1.18 (m, 38H), 0.92-0.83 (m, 6H)

^{13}C NMR (101 MHz, Chloroform-d) δ 129.9, 32.04, 32.0, 29.8, 29.7, 29.6, 29.5, 29.4, 29.39, 29.35, 27.3, 22.8, 14.2

Synthesis of *Z*-9 C_{25} (9)

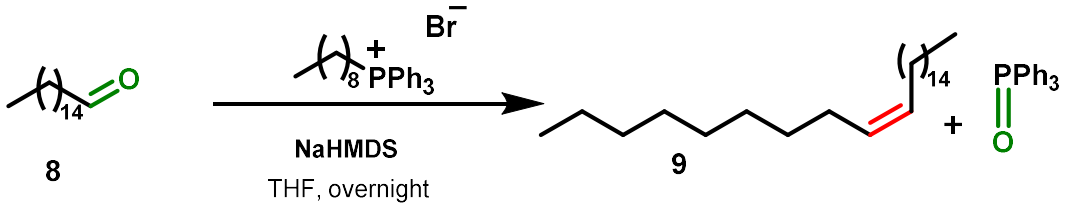

A 50 mL oven dried round bottom flask was equipped with magnetic stir bar and argon balloon. In the flask, (1-nonyl) triphenylphosphonium bromide (1.4 g, 3.1 mmol) and THF (10 mL) were added and stirred. A solution of NaHMDS (2M in THF, 1.5 mL) was added and stirred. The solution is stirred at room temperature for 15 minutes then placed in an ice bath with brine to cool. Hexadecanal (**8**) (372 mg, 1.5 mmol,) was dissolved in THF (10 mL) and the solution was added dropwise to the flask over 10 minutes. The mixture was warmed slowly and stirred overnight. The mixture was concentrated in vacuo and purified by silica gel column chromatography (100% hexane) to obtain *Z*-9 C_{25} (**9**) as colorless oil (436 mg, 80%).

^{1}H NMR (400 MHz, Chloroform-d) δ 5.33 (t, *J* = 7.4 Hz, 2H), 2.07-2.92 (m, 4H), 1.43-1.14 (m, 38H), 0.91-9.82 (m, 6H)

^{13}C NMR (101 MHz, Chloroform-d) δ 129.9, 32.0, 29.9, 29.8, 29.7, 29.6, 29.63, 29.5, 29.4, 27.3, 22.7, 14.2.

Synthesis of *Z*-7 C_{27} (12)

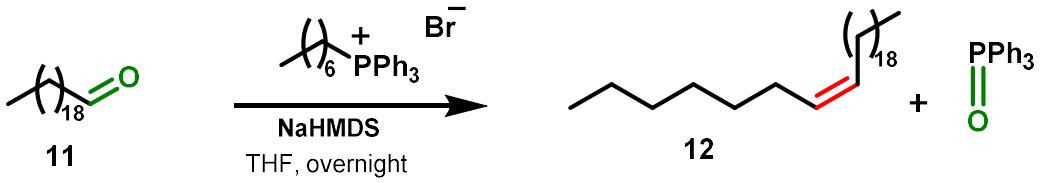

A 50 mL oven dried round bottom flask was equipped with magnetic stir bar and argon balloon. In the flask, (1-heptyl) triphenylphosphonium bromide (3.8 g, 8.6 mmol) and THF (20 mL) were added and stirred. A solution of NaHMDS (2M in THF, 4.3 mL) was added and stirred. The solution is stirred at room temperature for 15 minutes then placed in an ice bath with brine to cool. Eicosanal (**11**) (1.3 g, 4.3 mmol) was dissolved in THF (10 mL) and the solution was added dropwise to the flask over 10 minutes. The mixture was warmed slowly and stirred overnight. The mixture was concentrated in vacuo and purified by silica gel column chromatography (100% hexane) to obtain *Z*-7 C_{27} (**12**) as colorless oil (1.0 g, 65% yield).

^{1}H NMR (400 MHz, Chloroform-d) δ 5.34 (t, J = 7.4 Hz, 2H), 2.06-1.97 (m, 4H), 1.43-1.17 (m, 42H), 0.94-0.83 (m, 6H)

^{13}C NMR (101 MHz, Chloroform-d) δ 129.9, 32.7, 32.0, 31.8, 29.9, 29.8, 29.7, 29.6, 29.5, 29.4, 29.2, 29.1, 28.9, 27.3, 22.8, 22.7, 14.2.

Synthesis of *Z*-9 C_{27} (16)

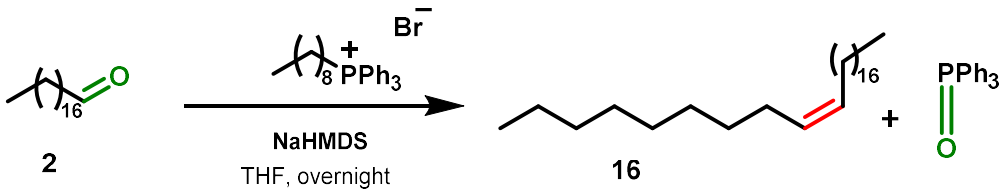

A 100 mL oven dried round bottom flask was equipped with magnetic stir bar and argon balloon. In the flask, (1-nonyl) triphenylphosphonium bromide (5.5 g, 11.7 mmol) and THF (25 mL) were added and stirred. A solution of NaHMDS (2M in THF, 4.9 mL) was added and stirred. The solution is stirred at room temperature for 30 minutes then placed in an ice bath with brine to cool. Octadecanal (**2**) (1.6 g, 5.8 mmol,) was dissolved in THF (15 mL) and the solution was added dropwise to the flask over 10 minutes. The mixture was warmed slowly and stirred overnight. The mixture was concentrated in vacuo and purified by silica gel column chromatography (100% hexane) to obtain *Z*-9 C_{27} (**16**) as colorless oil (1.9 g, 88% yield).

^{1}H NMR (400 MHz, Chloroform-d) δ 5.36 (t, *J* = 7.4 Hz, 2H), 2.09-1.97 (m, 4H), 1.45-1.19 (m, 42H), 0.92-0.84 (m, 6H).

^{13}C NMR (101 MHz, Chloroform-d) δ 129.9, 32.7, 32.1, 32.0, 29.9, 29.85, 29.81, 29.7, 29.6 29.5, 29.4, 29.3, 27.3, 22.8, 14.2.

Synthesis of 19

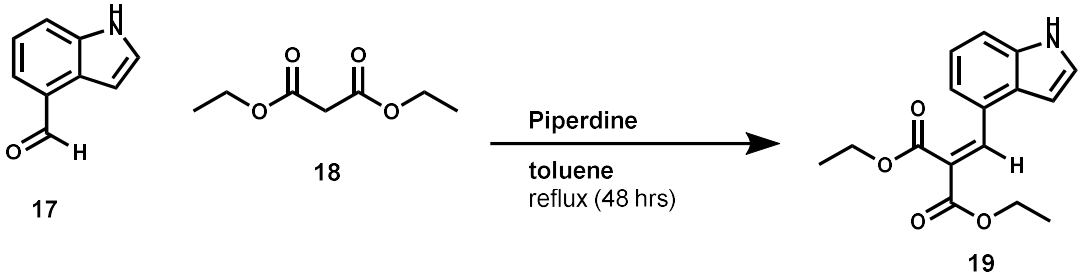

A 50 mL round bottom flask was equipped with condenser and argon balloon and submerged in an oil bath. Indole-4 carboxaldehyde (**17**) (600 mg, 0.5 mmol) and toluene (10 mL)

was added to the flask and stirred. Temperature was set to 110 °C. Diethyl malonate (**18**) (309.5 mg, 0.50 mmol) and piperidine (0.02 mL) was added to the flask, respectively. The mixture was refluxed for 2 days. The mixture was concentrated in vacuo and purified by silica gel column chromatography (25% ethyl acetate/hexane, 30% ethyl acetate/hexane) to obtain (**19**) (218 mg, 49 % yield).

^{1}H NMR (400 MHz, Chloroform-d) δ 10.25 (d, 1H), 8.23 (s, 1H), 7.66 (m, 2H), 7.46 (d, *J* = 8.2 Hz, 1H), 7.16 (t, *J* = 7.9 Hz, 1H), 6.73 (t, *J* = 3.0 Hz, 1H), 4.31 (m, 4H), 1.33 (m, 6H).

Synthesis of 20

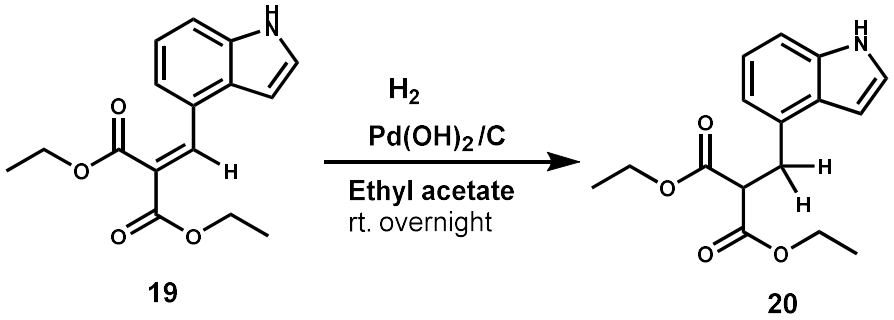

19 **20**

A 50 mL two-necked round bottom flask and hydrogen balloon were prepared. Ethyl acetate (7 mL) was used to dissolve compound **15** (218mg, 0.8 mmol) and added to the flask. $Pd(OH)_2$ /C (21 mg, 20%) and ethyl acetate (2 mL) was added to the flask. The air was vacuumed out of the flask until the solution bubbled and hydrogen gas was introduced to the flask. The process was repeated 3-4 times and hydrogen balloon was kept on the flask. The mixture was stirred for 24 hrs at room temperature. The mixture was vacuum filtered using silica to get rid of the $Pd(OH)_2$ /C. The product was concentrated in vacuo to give compound **16** (132 mg, 60% yield).

^{1}H NMR (400 MHz, Chloroform-d) δ 7.26 (d, *J* = 7.8 Hz, 1H), 7.20 (t, *J* = 2.9 Hz, 1H), 7.09 (d, *J* = 7.7 Hz, 1H), 6.94 (t, *J* = 7.2 Hz, 1H), 6.60 (d, *J* = 2.6 Hz, 1H), 4.20 (m, 4H), 3.84 (t, *J* = 7.6 Hz, 1H), 3.51 (d, *J* = 7.6 Hz, 2H), 1.21 (m, 6H).

Synthesis of 21

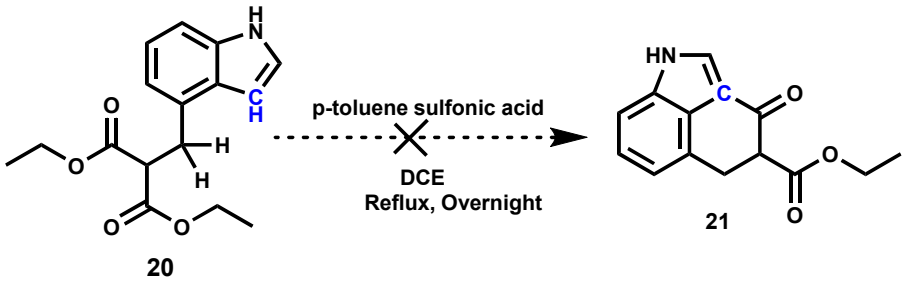

A 25 mL round bottom flask was obtained and equipped with argon balloon. Compound **16** (60.0 mg) was dissolved in DCE (2 mL) and added to the flask. p-TSA and remaining DCE (8 mL) were added to the flask. The mixture was refluxed overnight at 80 degree Celsius.

REFERENCES

[1] Rosenkranz, P.; Aumeier, P.; Ziegelmann, B. Biology and Control of Varroa destructor. *Journal of Invertebrate Pathology*. **2010**, 103, S96-SI 19.

[2] Khan, A. K.; Ghramh, A. H. An investigation of the efficacy of hygienic behavior of various honeybee (*Apis mellifera*) races toward *Varroa destructor* (Acari: *Varroidae*) mite infestation. *Journal of King Saud University – Science*. **2021**, 33, 101-393.

[3] Ifantidis, M. D. Some aspects of the process of *Varroa jacobsoni* mite entrance into honeybee (*Apis mellifera*) brood cells. *Apidologie*. **1988**, 19, 387-396.

[4] Ramsay, S.; Ochoa, R.; Bauchan, G.; Gulbronson, C.; Mowery, J. *Varroa destructor* feeds primarily on honeybee fat body tissue and not hemolymph. *Proceedings of the National Academy of Sciences*, **2019**, 116 (5), 1792-1801

[5] Bailey, L.; Ball, B. Honeybee Pathology. *Academic Press*. **1991**, 3-7.

[6] De Miranda, J. R.; Genersch, E. Deformed Wing Virus. *Journal of Invertebrate Pathology*. **2010**, 103, S48-S61.

[7] Newton, D. C.; Ostasiewski, N. J. Jr. A simplified bioassay for behavioral resistance to American foulbrood in honeybees (*Apis mellifera*). *The American Bee Journal.* **1986,** 126, 278–281.

[8] Leclercq, G.; Gengler, F. N.; Blacquière, T. Bioassays to quantify hygienic behavior in honeybee (*Apis mellifera L.*) colonies: a review. *Journal of Apicultural Research*. **2018**, 57, 663–673.

[9] Wagoner, K.; Spivak, M.; Hefetz, A.; Reams, T.; Rueppell, O. Stock-specific chemical brood signals are induced by *Varroa* and Deformed Wing Virus and elicit hygienic response in the honeybee. *Nature*. **2019**, 9, 8753

[10] Annoscia, D.; Del Piccolo, F.; Nazzi, F. How does the mite *Varroa destructor* kill the honeybee *Apis mellifera*? Alteration of cuticular hydrocarbons and water loss in infested honeybees. *Journal of Insect Physiology*. **2012**, 58, 1548-1555.

[11] Blomquist, G. J.; Vogt, R. G. Insect pheromone biochemistry and molecular biology: The biosynthesis and detection of pheromones and plant volatiles. *Elsevier Academic Press*, San Diego, CA. **2003**, 3-18.

[12] Soroker, V.; Hefetz, A. Hydrocarbon site of synthesis and circulation in the desert ant *Cataglyphis niger*. *Journal of Insect Physiology*. **2000** 46, 1097-1102.

[13] Memmott, J.; Waser, N. M.; Price, M. V. Tolerance of pollination networks to species extinctions. Proceedings of the Royal Society of London. *Series B: Biological Sciences*. **2004**, 271, 2605-2611.

[14] Dani, F. R.; Jones, G. R.; Corsi, R. S.; Beard, D. P.; Turillazzi, S. Nestmate recognition cues in the honeybee: differential importance of cuticular alkanes and alkenes. *Chemical Senses*. **2005**, 30, 477–489.

[15] Wagoner, K. M.; Millar, J. G.; Schal, C.; Rueppell, O. Cuticular pheromones stimulate hygienic behavior in the honeybee (*Apis mellifera*). *Scientific Reports.* **2020**, 10, 7132.

[16] Blomquist, G. J.; Howard, R. Pheromone biosynthesis in social insects. *Academic Press*. **2003**, 323–340.

[17] Wagoner, K.; Millar, J. G.; Keller, J.; Bello, J.; Waiker, P.; Schal, C.; Spivak, M.; Rueppell, O. Hygiene-Eliciting Brood Semiochemicals as a Tool for Assaying Honeybee

(*Hymenoptera: Apidae*) Colony Resistance to *Varroa* (*mesostigmata: Varroidae*). *Journal of Insect Science*, **2021**, 21, 1-13.

[18] Brahmbhatt, V. V. Quantification of pentafluorobenzyl oxime derivatives of long chain aldehydes by GC-MS analysis. *Lipids.* **2008**, 43, 275-80.

[19] Seigler, D.S. Plant Secondary Metabolism. *Plant Growth Regulation.* **2001**, 34, 628.

[20] Gore, S.; Baskaran, S.; König, B. Fischer Indole Synthesis in Low Melting Mixtures *Organic Letters*. **2012**, 14, 4568-4571.

[21] Bartoli, G.; Bencivenni, G.; Dalpozzo, R. Organocatalytic Strategies for the Asymmetric Functionalization of Indoles. *Chemical Society Review*. **2010**, 39, 4449.

[22] Tasker, N. R.; Wipf, P. Biosynthesis, total synthesis, and biological profiles of Ergot. *Academic Press*. **2021,** 85, 1-112

[23] Rajat, M.; Mallojjala, S. C.; Wheeler, S. E. Chiral Phosphoric Acid Catalysis: From Numbers to Insights. *Chemical Society Review*. **2018**, 47, 1142-1158.

[24] Wilent, J.; Petersen, K. S. Enantioselective Desymmetrization of Diesters. *Journal of Organic Chemistry*. **2014**, 79, 2303–2307.

[25] Kelley, A. M.; Haywood, R. D.; White, J. C.; Petersen, K. S. Enantioselective Desymmetrizations of Diesters to Synthesize Fully Substituted Chiral Centers of 3,4-Dihydrocoumarins and Related Compounds. *Chemistry Select* **2020**, 5, 3018– 3022.

[26] Berdyshev, E. V. Mass spectrometry of fatty aldehydes. *Biochimica et Biophysica Acta (BBA) - Molecular and Cell Biology of Lipids.* **2011**. 1811 (11), 680-93.

[27] Robiette, R.; Richardson, J.; Aggarwal, V. K.; Harvey, J. *Journal of the American Chemical Society*. **2006** 128, 2394-2409.

.

APPENDIX A: NMR SPECTRA

The ^{1}H and ^{13}C nuclear magnetic resonance (NMR) spectra were plotted on a JEOL ECS 400 MHz spectrometer using $CDCl_3$ as a solvent at room temperature. The NMR chemical shifts (δ) are reported in ppm. Abbreviations for ^{1}H NMR: s = singlet, d = doublet, t = triplet, q = quartet, sept = septet, m = multiplet.

^{1}H NMR

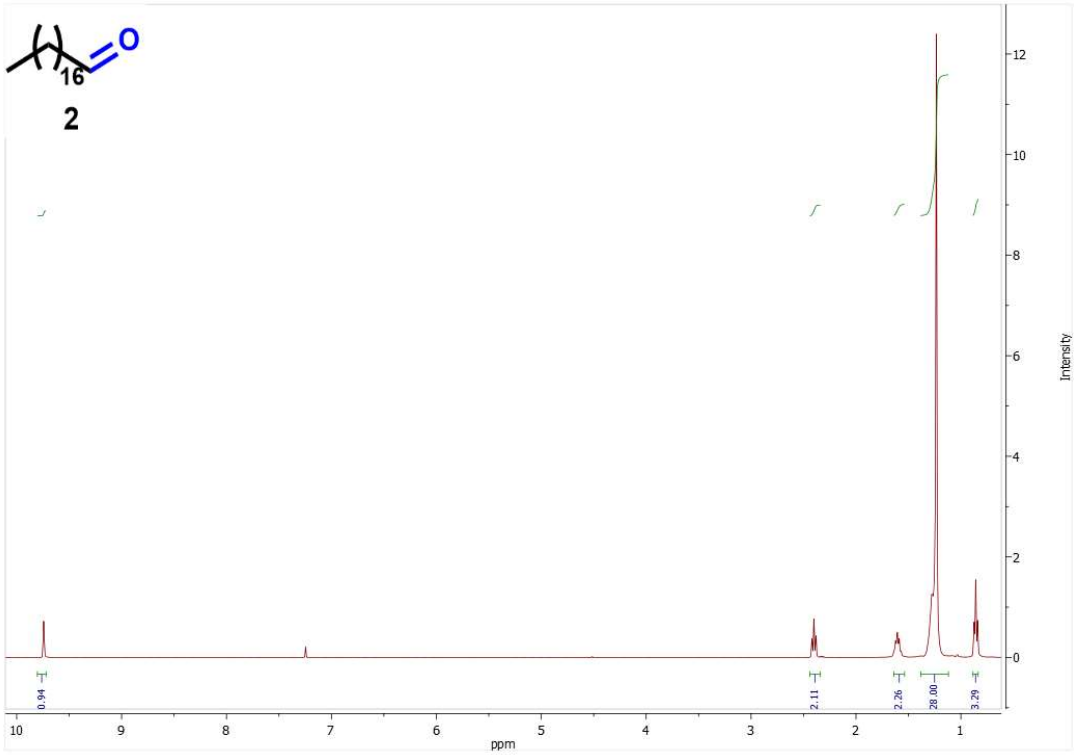
16
O
2
0.94
2.11
2.26
28.00
3.29
10
9
8
7
6
5
4
3
2
1
ppm
Intensity

^{1}H NMR

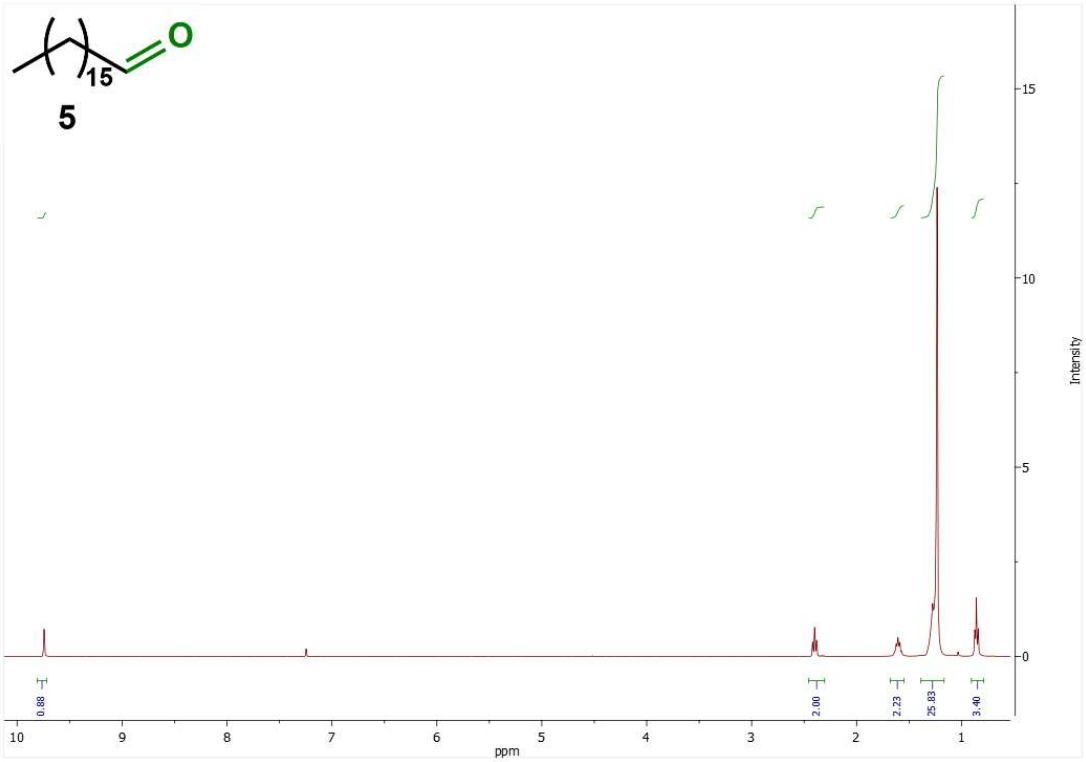
15
O
5
0.88
2.00
2.23
25.83
3.40
10
9
8
7
6
5
4
3
2
1
ppm
Intensity

^{1}H NMR

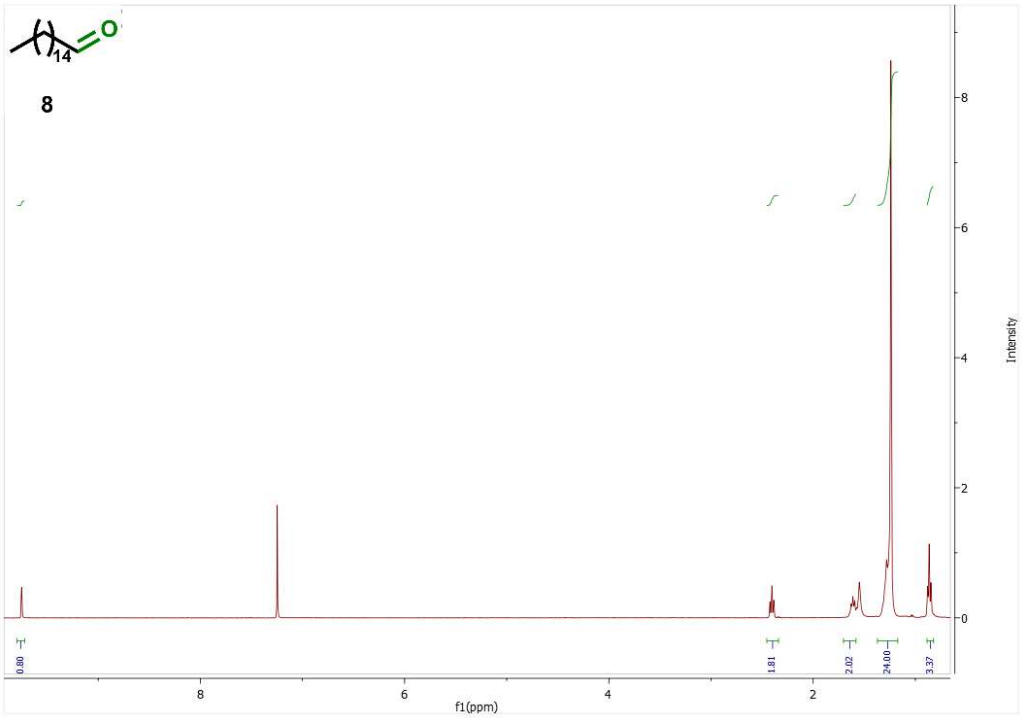
14
O
8
0.80
1.81
2.02
24.00
3.37
f1(ppm)
Intensity

^{1}H NMR

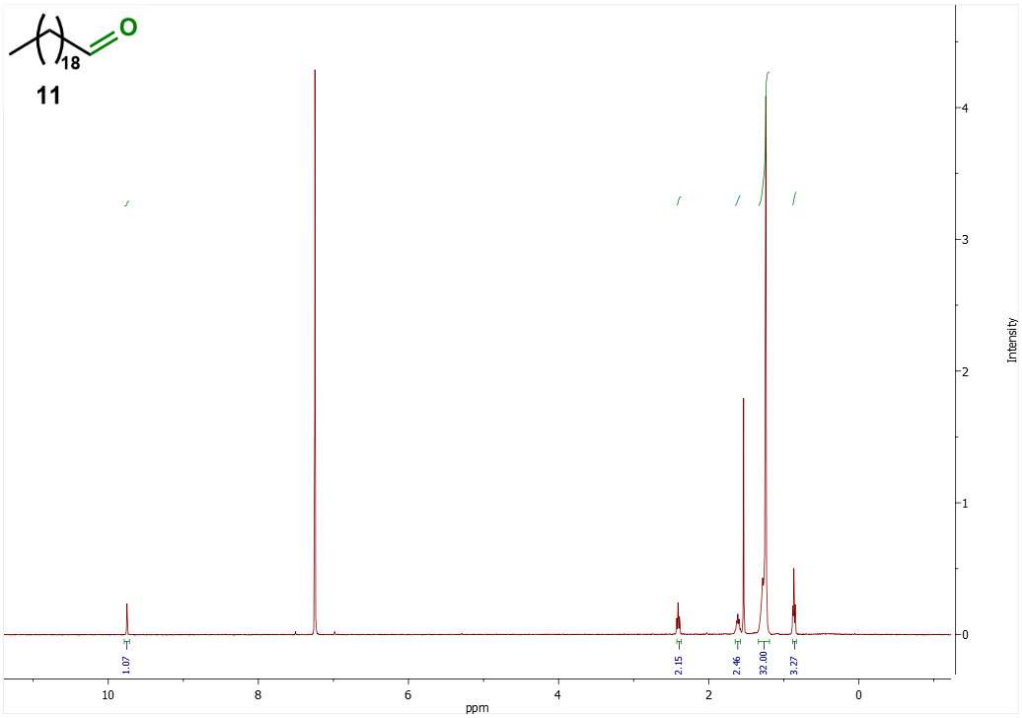
18
O
11
1.07
2.15
2.46
32.00
3.27
ppm
Intensity

^{1}H NMR

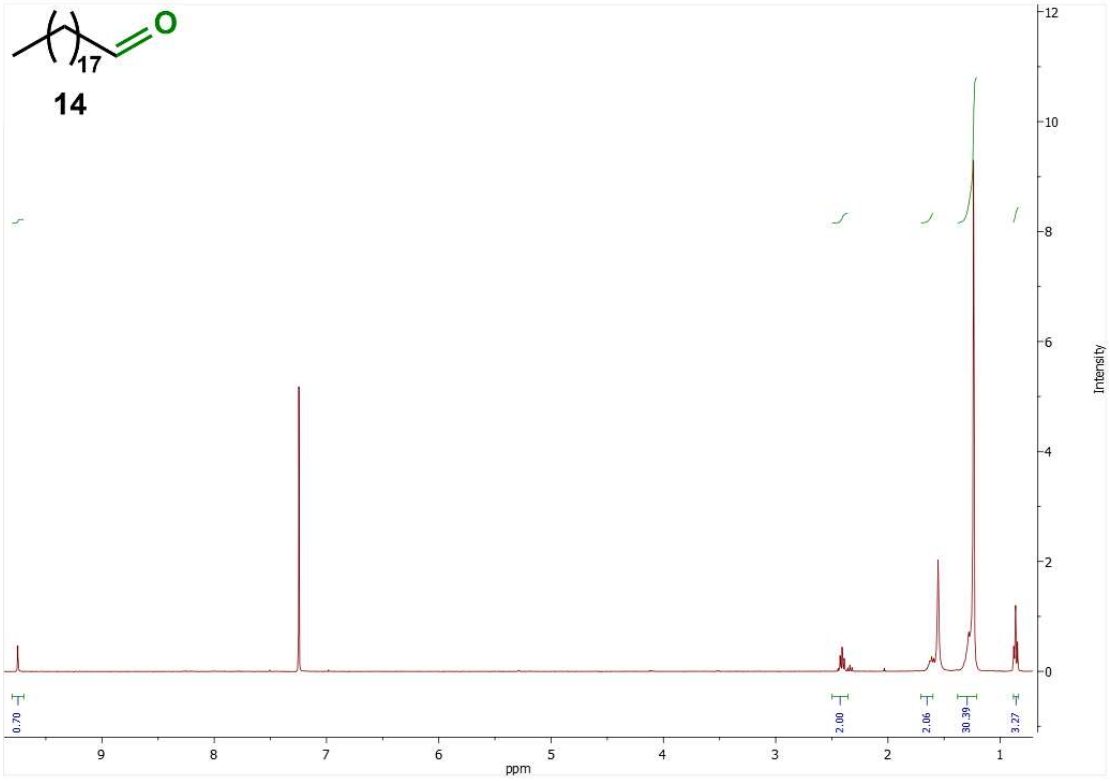
O
17
14
12
10
8
6
4
2
0
Intensity
0.70
2.00
2.06
30.39
3.27
9
8
7
6
5
4
3
2
1
ppm

^{1}H NMR

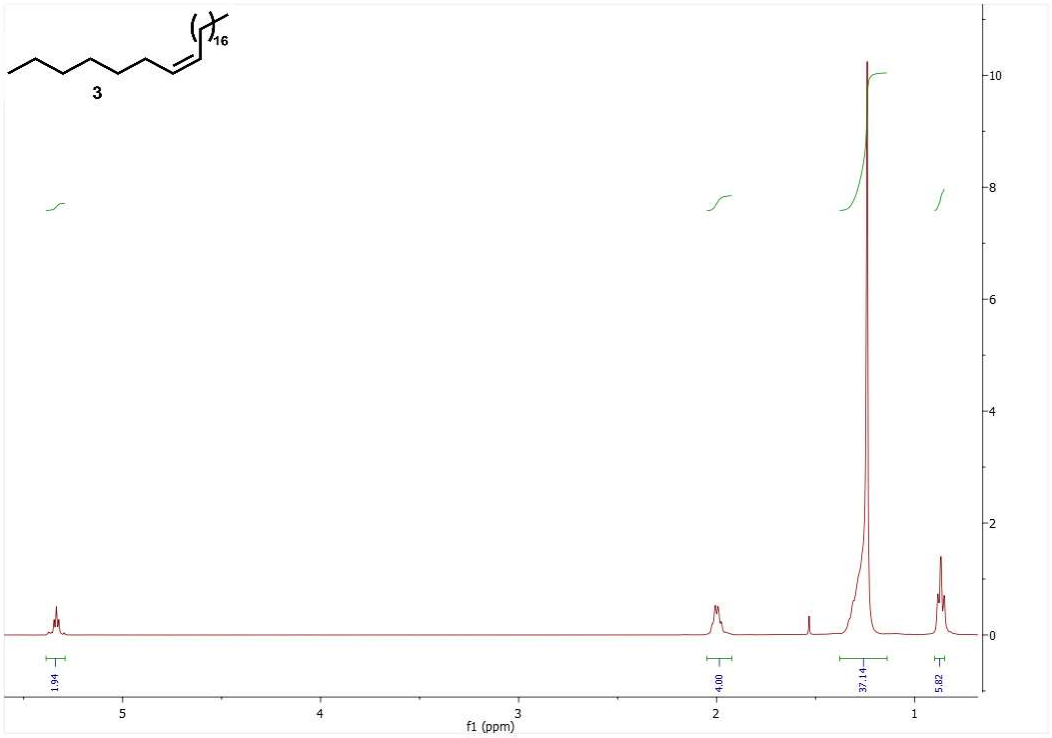

^{13}C NMR

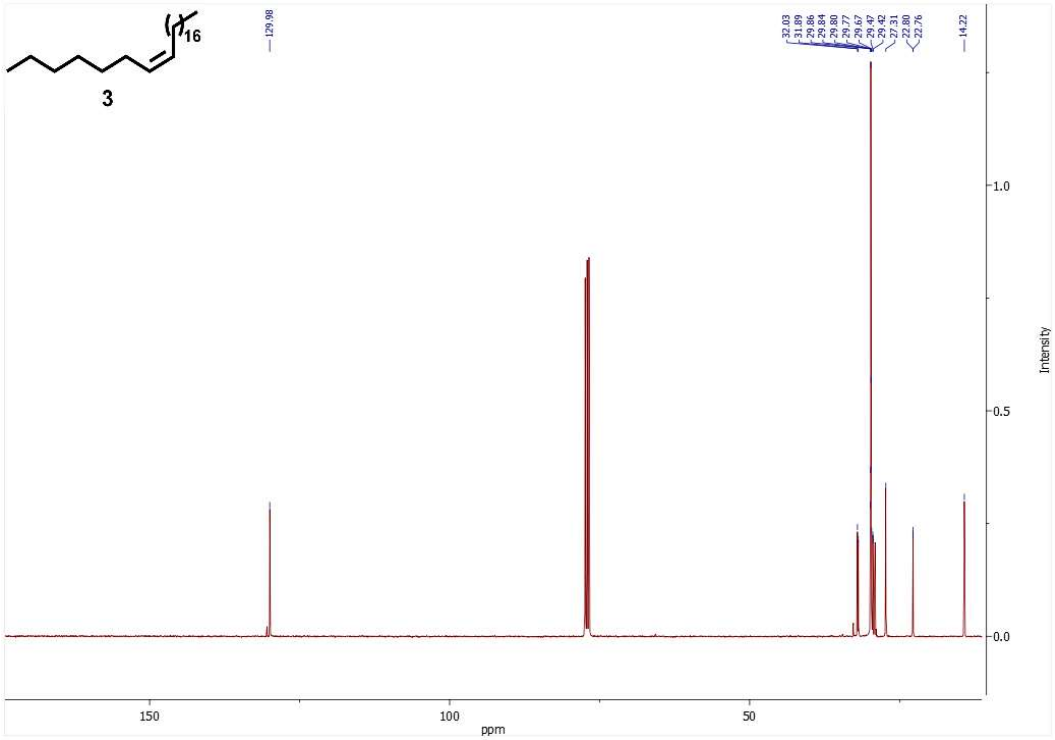

^{1}H NMR

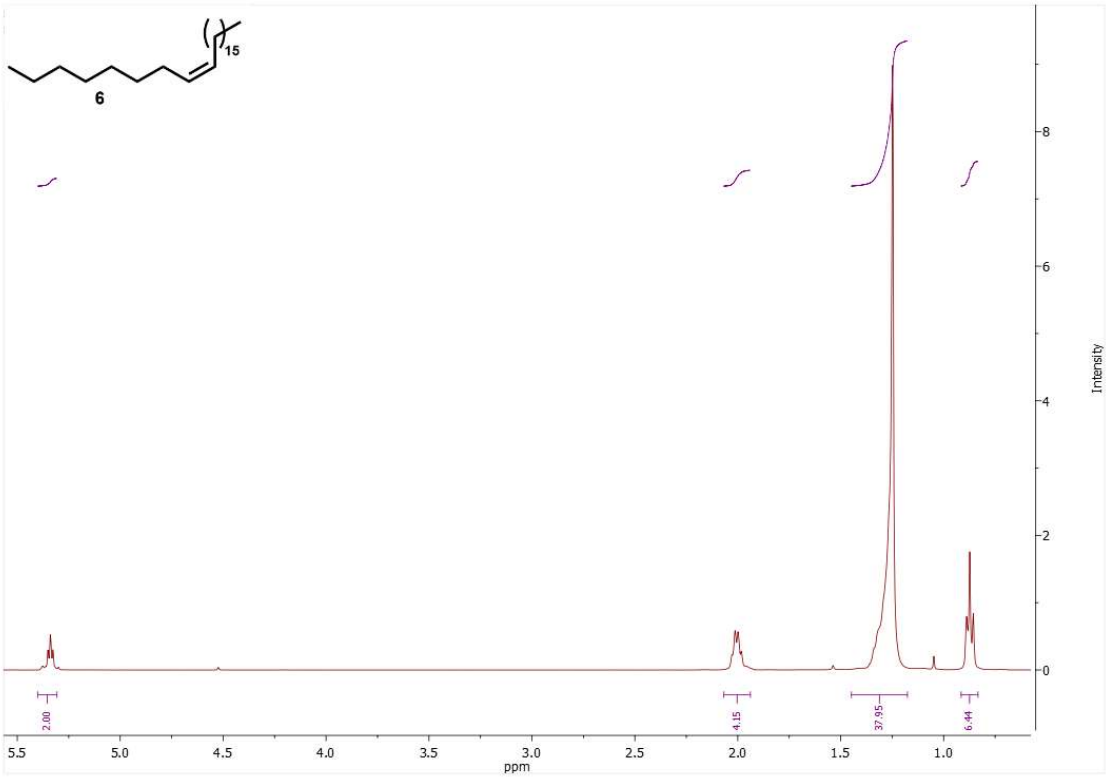

^{13}C NMR

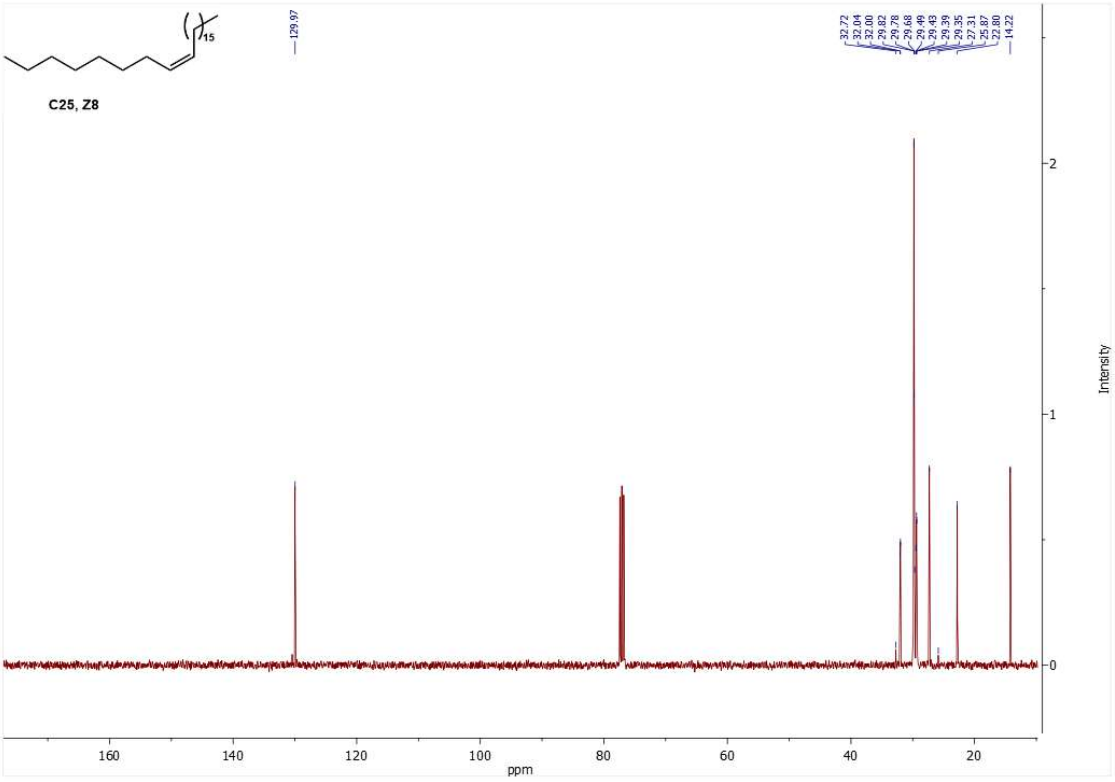

^{1}H NMR

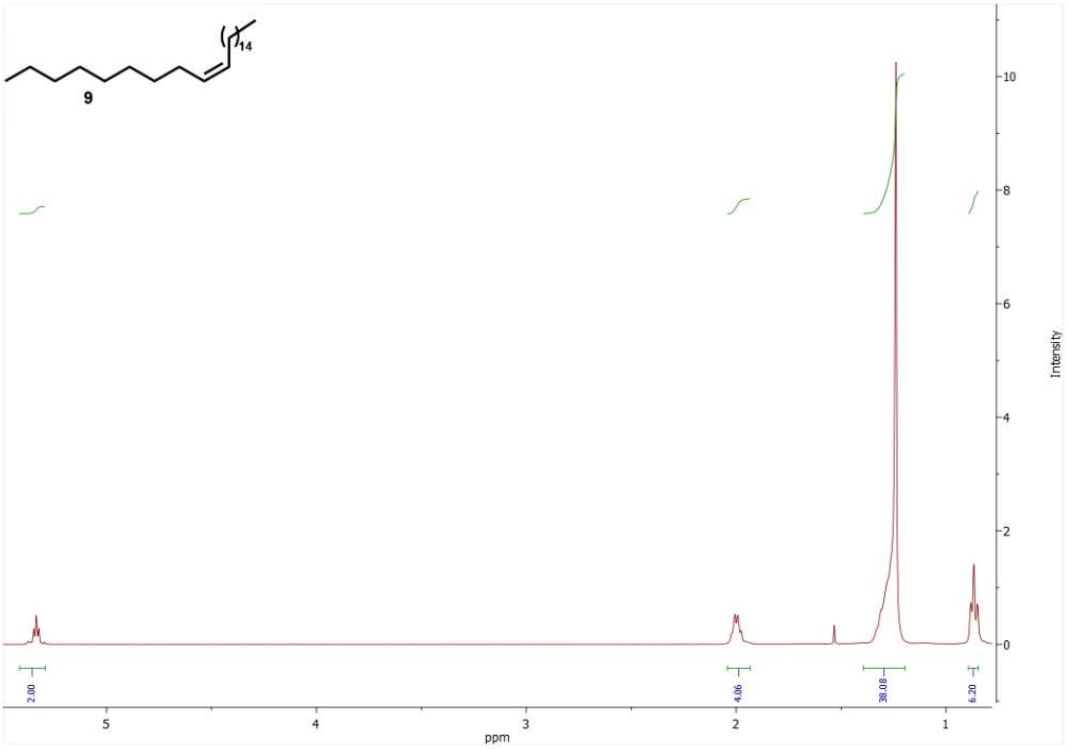

^{13}C NMR

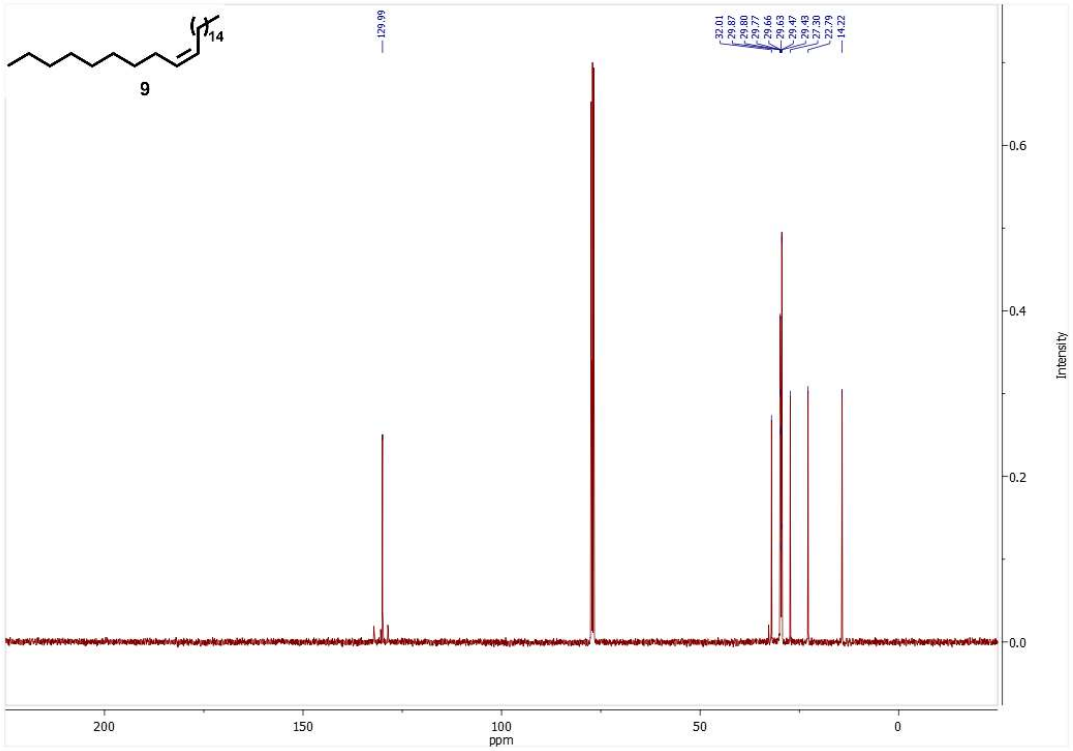

^{1}H NMR

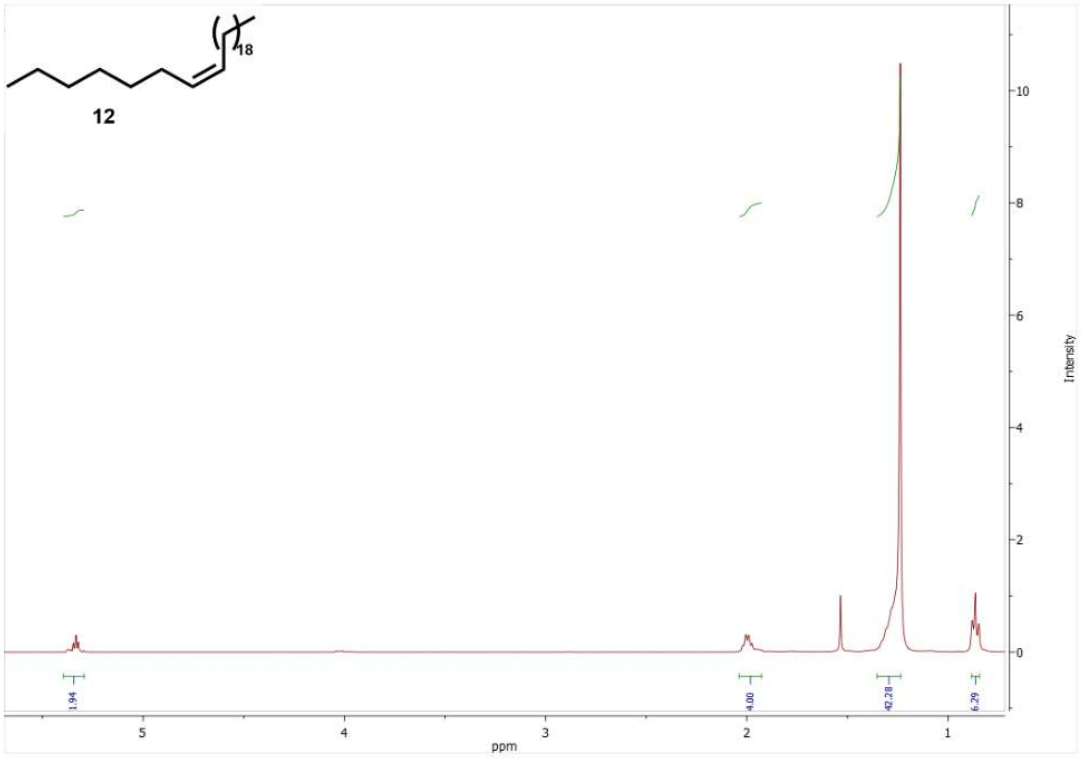

^{13}C NMR

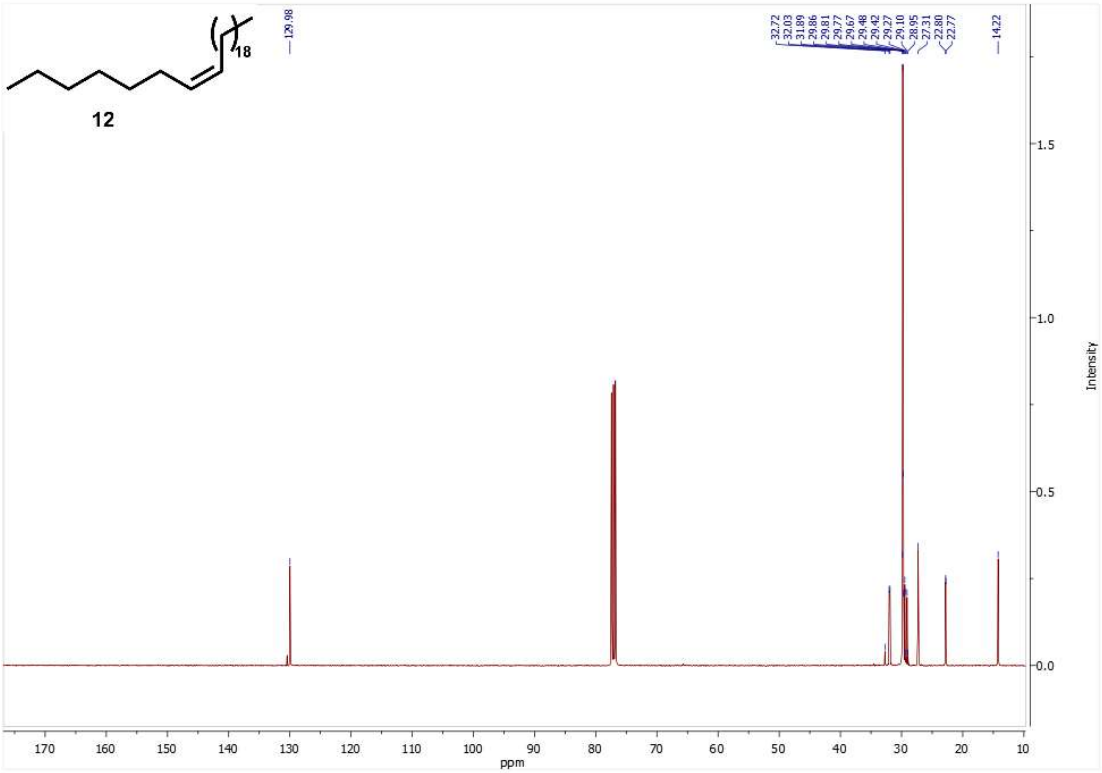

^{1}H NMR

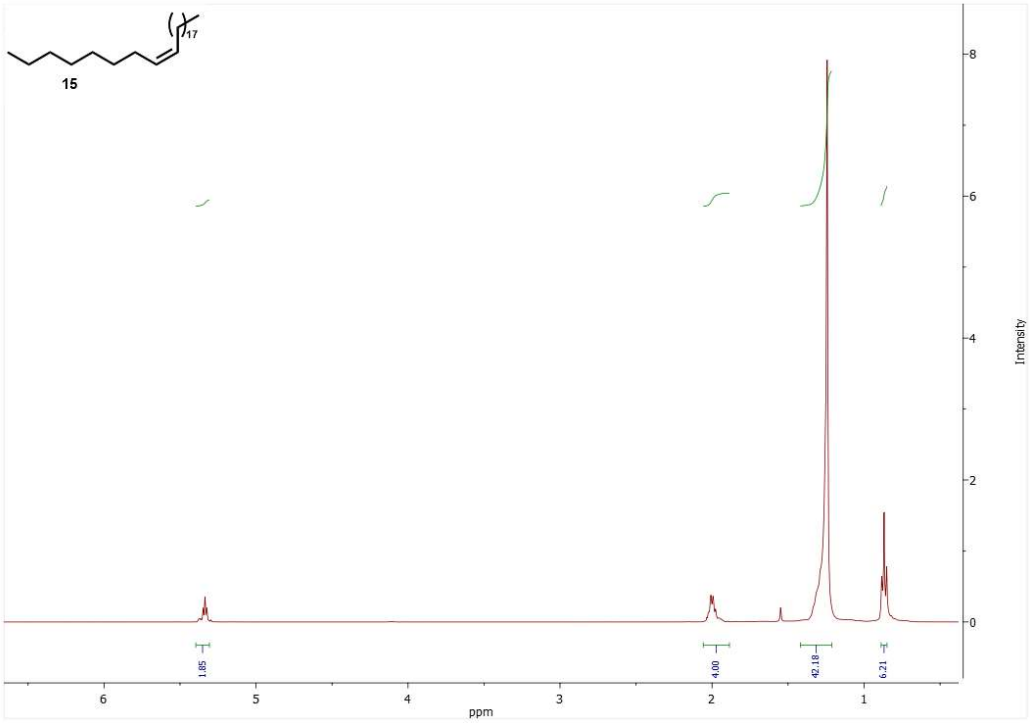

^{13}C NMR

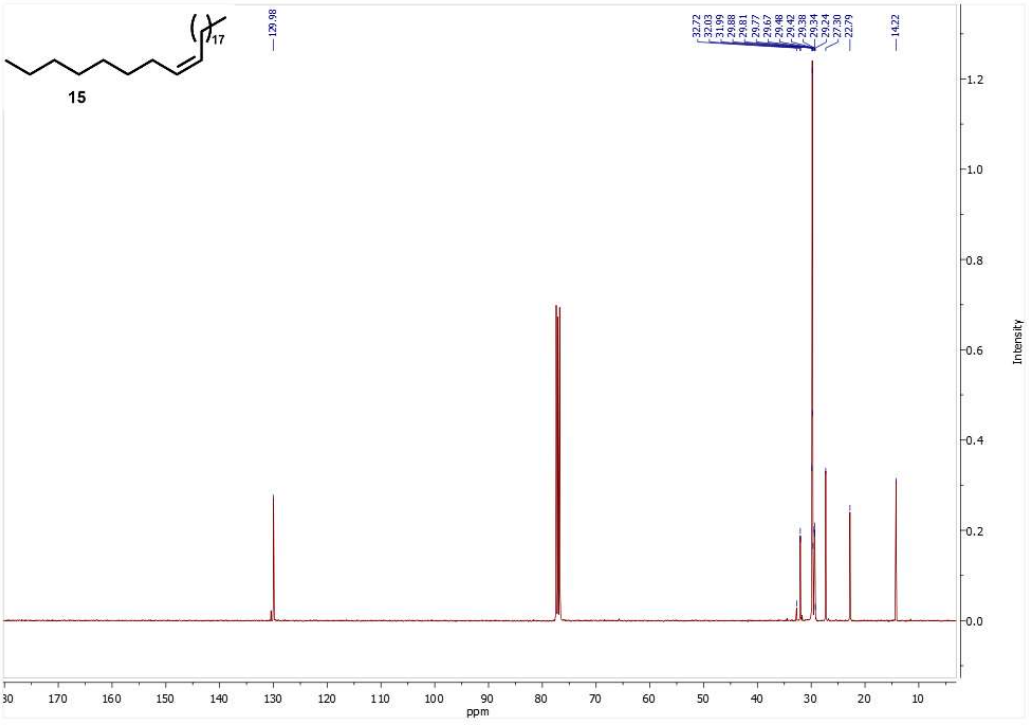

^{1}H NMR

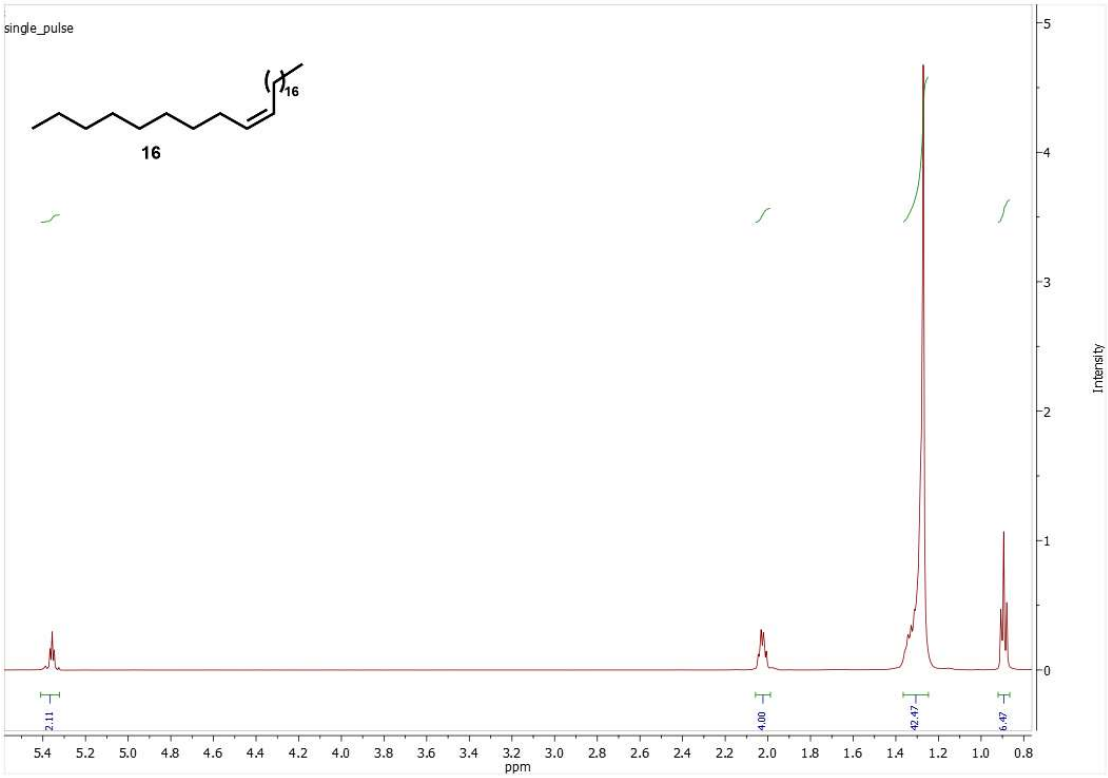

^{13}C NMR

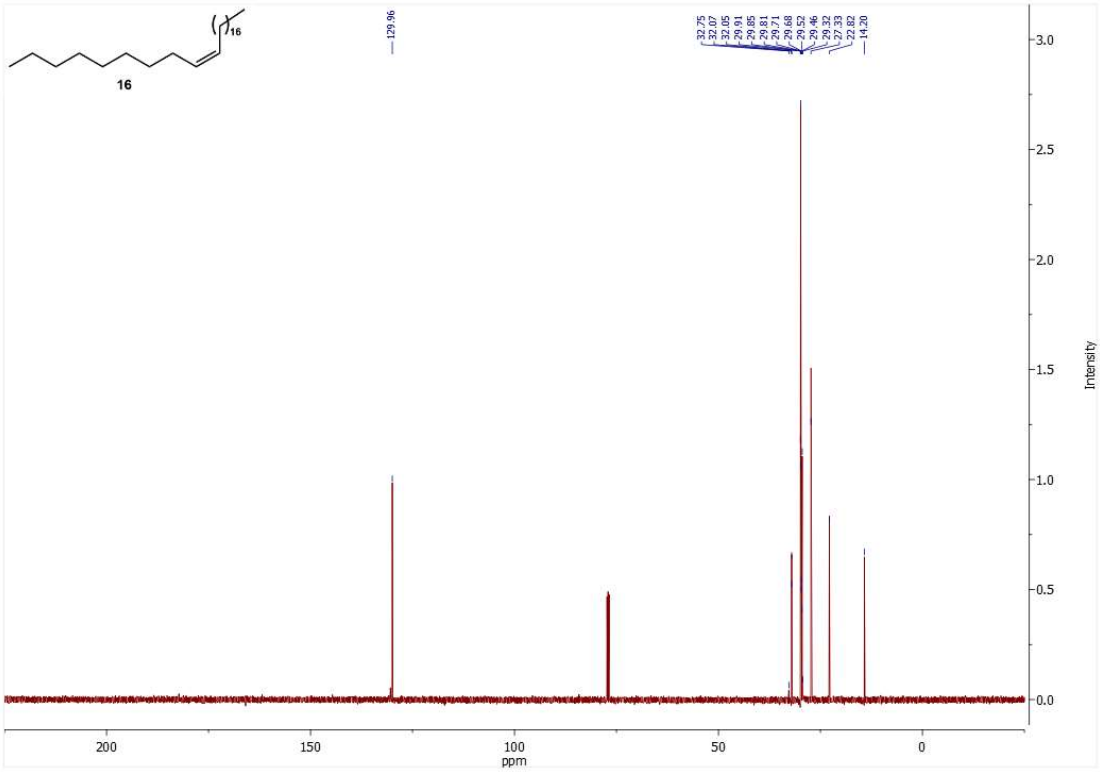

^{1}H NMR

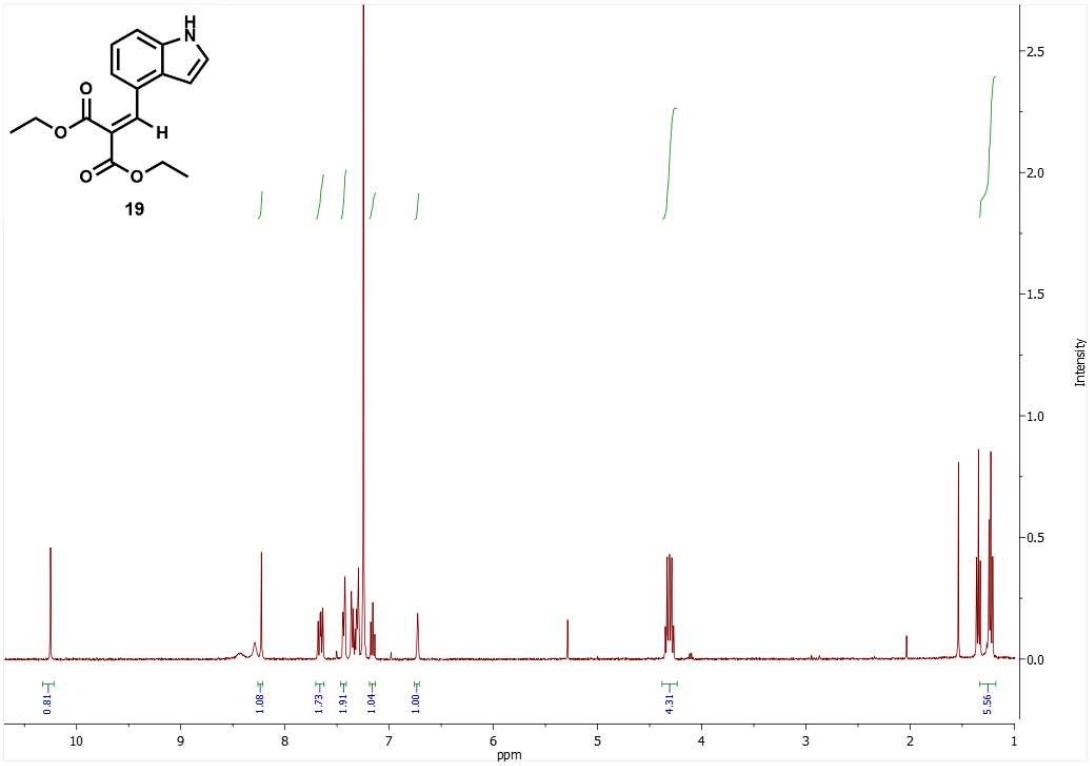
19
0.81
1.08
1.73
1.91
1.04
1.00
4.31
5.56
ppm
Intensity

^{1}H NMR

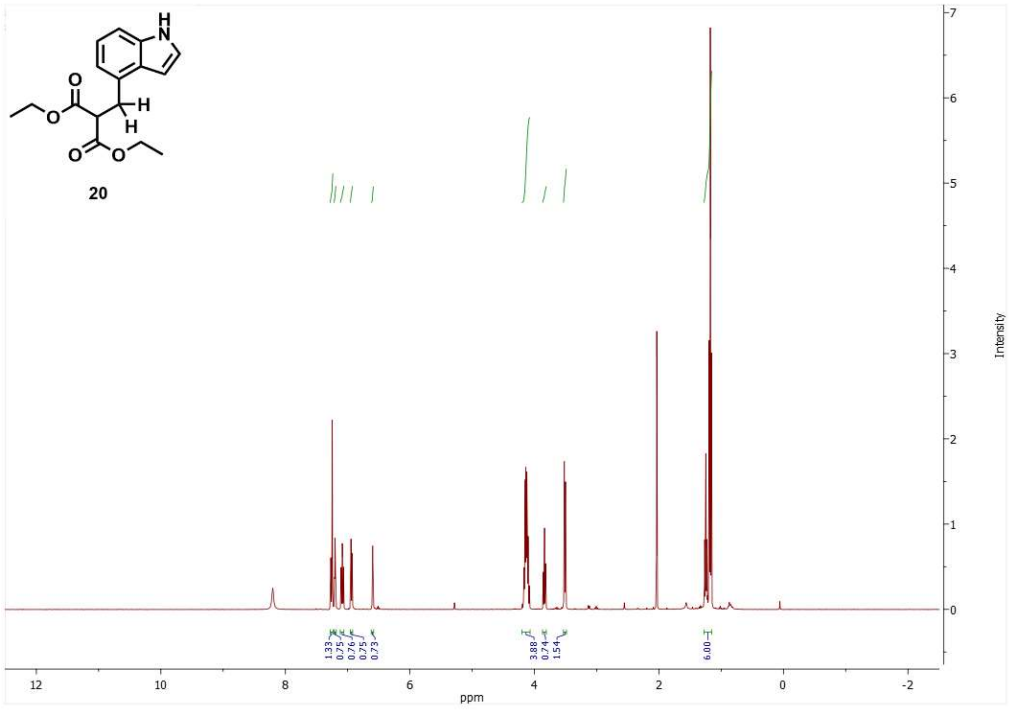
20
1.33
0.75
0.76
0.75
0.73
3.88
0.74
1.54
6.00
ppm
Intensity

APPENDIX B: GAS CHROMATOGRAPHY MASS SPECTROMETRY

GCMS-mass spectrum were obtained using GC-MS with single quadrupole mass analyzer (QP2010S, Shimadzu equipped with electron impact ionization. The mass range of m/z 500 and unit resolution was used. Methods from Wagoner et.al (2019) were used to obtain the spectrum.[9]

Z-7 C_{25}

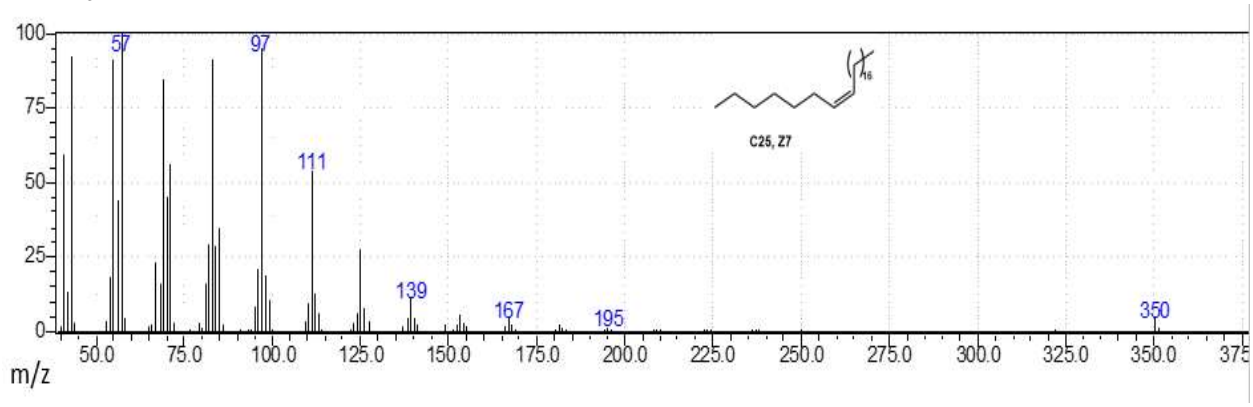

Z-8 C_{25}

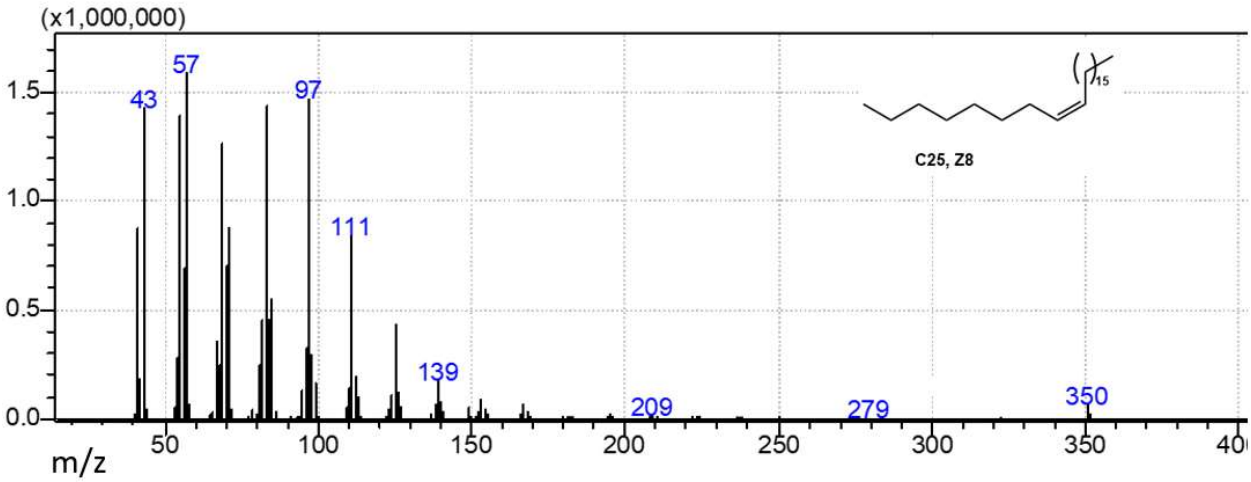

Z-9 C_{25}

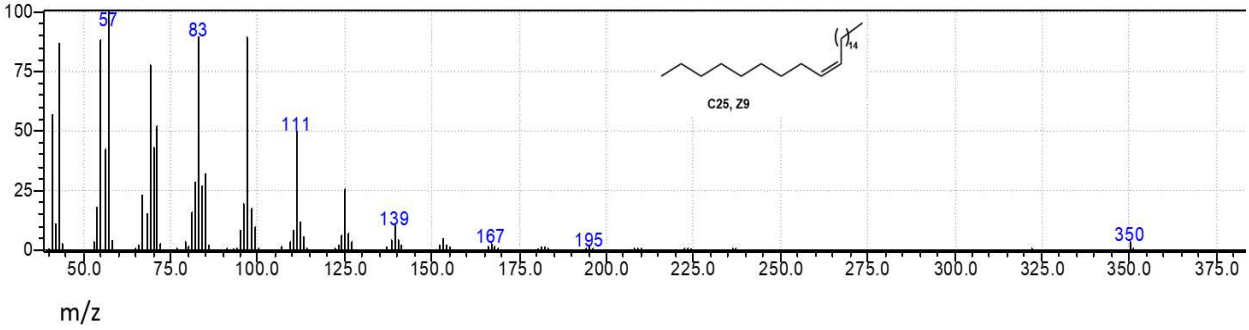

Z-7 C_{27}

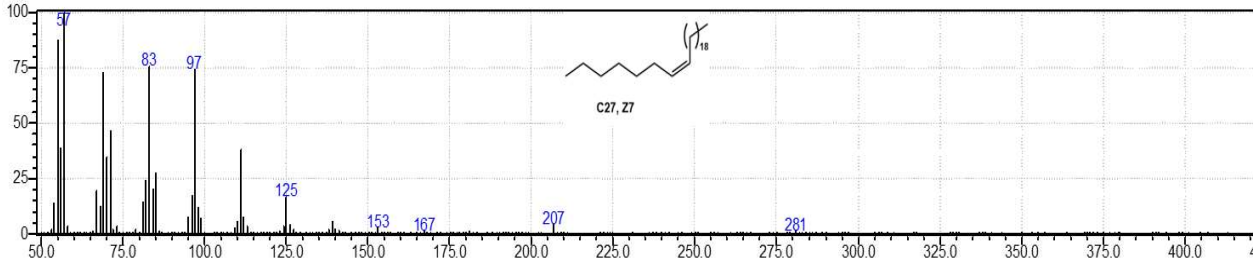

Z-8 C_{27}

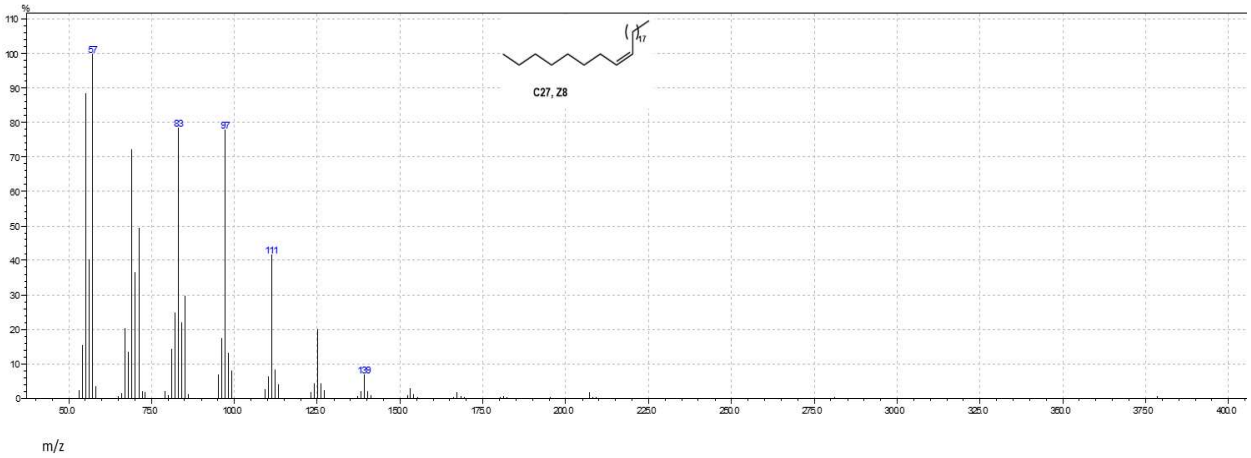

Z-9 C_{27}

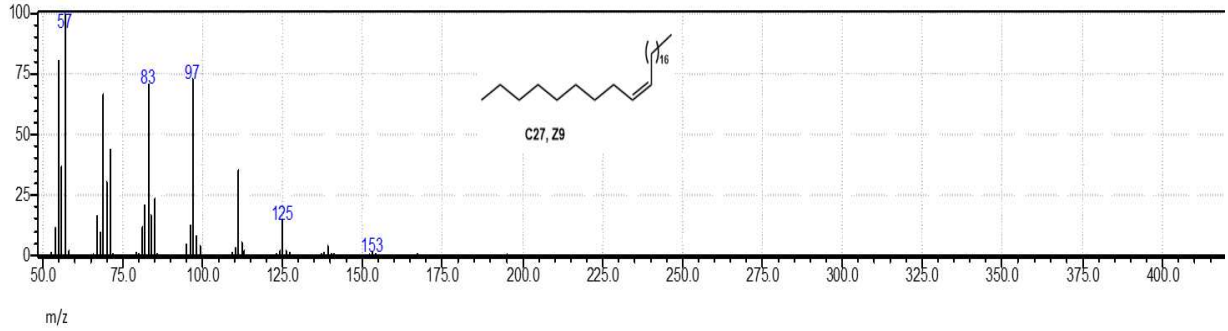

Byproduct of *Z*-8 C_{25} or *Z*-8 C_{27}

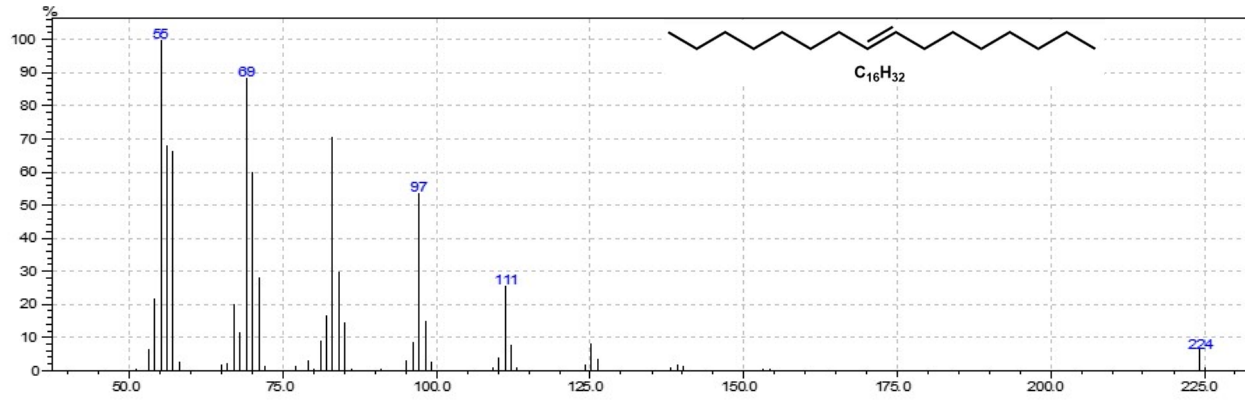

Byproduct of *Z*-7 C_{25} or *Z*-7 C_{27}

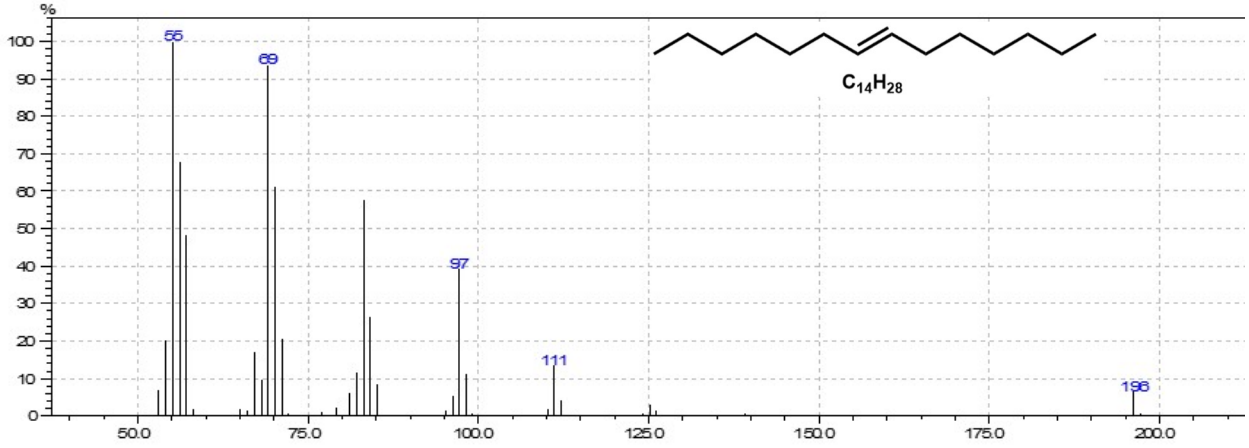

APPENDIX C: GAS CHROMATOGRAPHY

GC chromatograms were obtained using an Agilent 7890A. The chiral column used was a Supelco Betadex 110 Fused Silica Capillary Column (30m x 0.25mm x 0.25 μm).

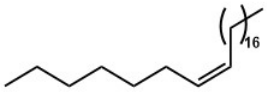

C25, Z7

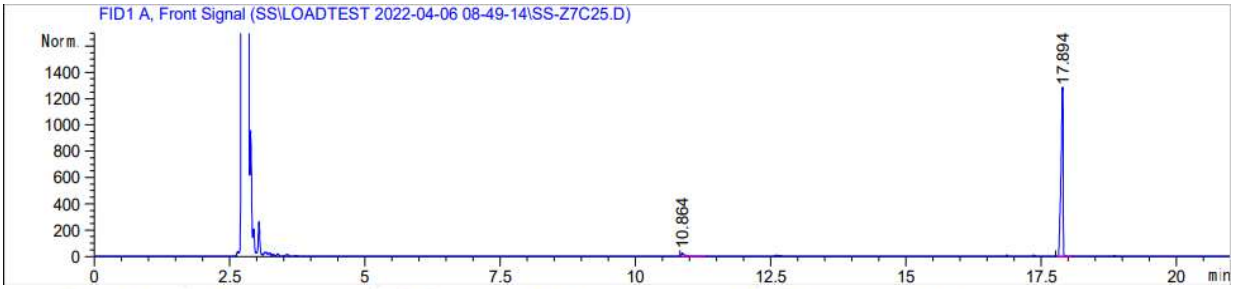

Peak #	RetTime [min]	Type	Width [min]	Area [pA*s]	Height [pA]	Area %
1	10.864	VB	0.0501	88.26133	23.89940	2.59878
2	17.894	VB	0.0370	3307.99487	1286.92834	97.40122

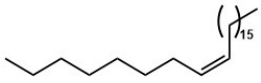

C25, Z8

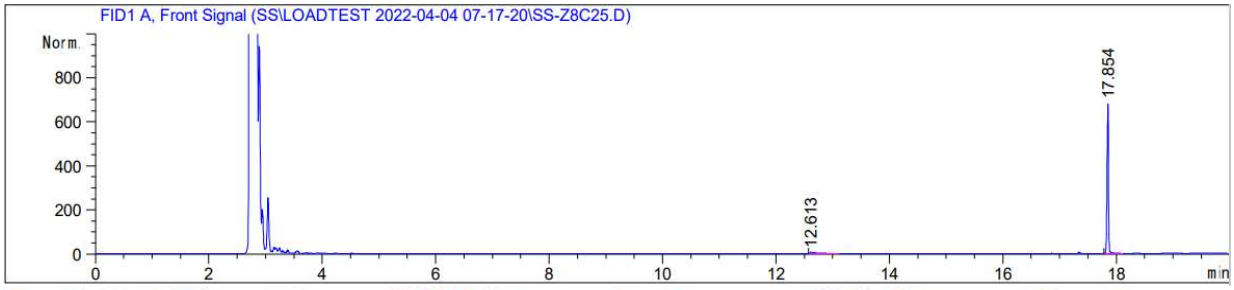

Peak #	RetTime [min]	Type	Width [min]	Area [pA*s]	Height [pA]	Area %
1	12.613	BB	0.1055	46.56022	5.51199	3.69000
2	17.854	BB	0.0278	1215.23608	681.04169	96.31000

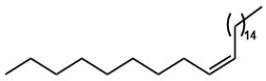

C25, Z9

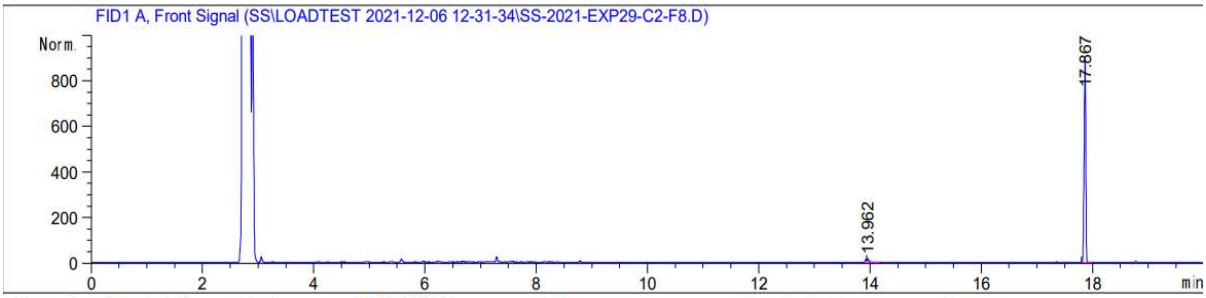

Peak #	RetTime [min]	Type	Width [min]	Area [pA*s]	Height [pA]	Area %
1	13.962	VB	0.0341	39.85201	16.54704	2.06749
2	17.867	BV	0.0317	1887.70203	892.53265	97.93251

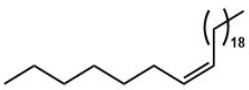

C27, Z7

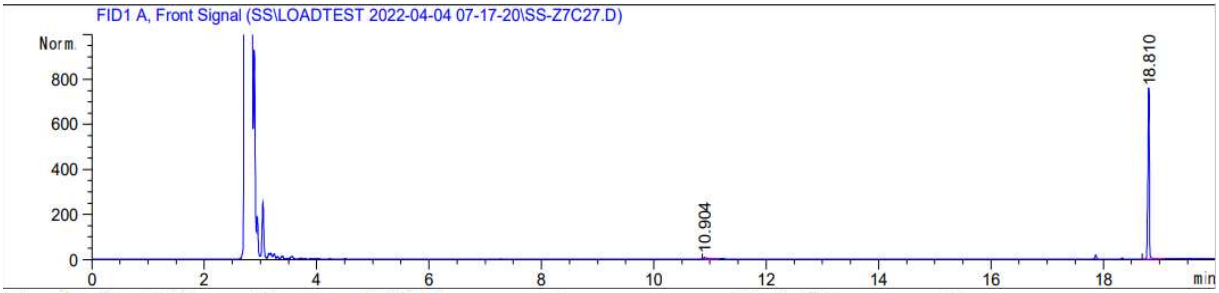

Peak #	RetTime [min]	Type	Width [min]	Area [pA*s]	Height [pA]	Area %
1	10.904	BV	0.0716	29.77489	5.45907	2.19590
2	18.810	VB	0.0253	1326.15479	760.71063	97.80410

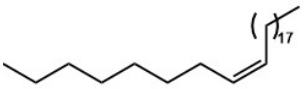

C27, Z8

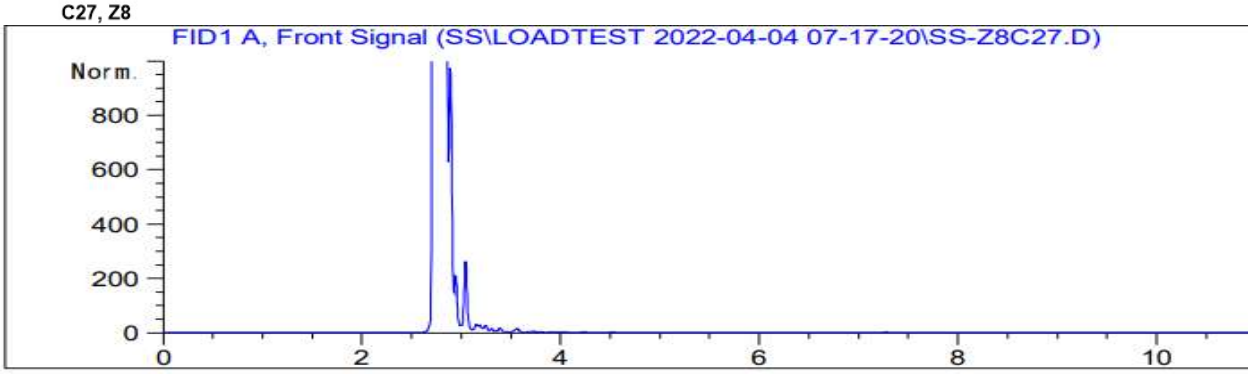

Peak #	RetTime [min]	Type	Width [min]	Area [pA*s]	Height [pA]	Area %
1	12.586	BB	0.1037	59.00978	7.34487	2.96129
2	18.800	BB	0.0264	1933.69336	1007.21643	97.03871

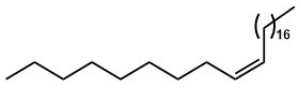

C27, Z9

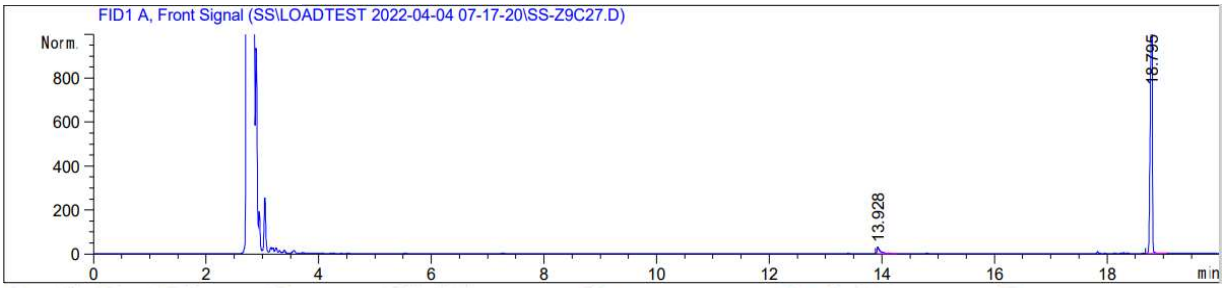

Peak #	RetTime [min]	Type	Width [min]	Area [pA*s]	Height [pA]	Area %
1	13.928	BB	0.0508	113.23059	30.18566	3.43205
2	18.795	VV	0.0360	3185.97949	1328.60071	96.56795